V.M.Chechetkin
Keldysh IPM RAS

High-Energy Neutrinos and Type-II Supernovae

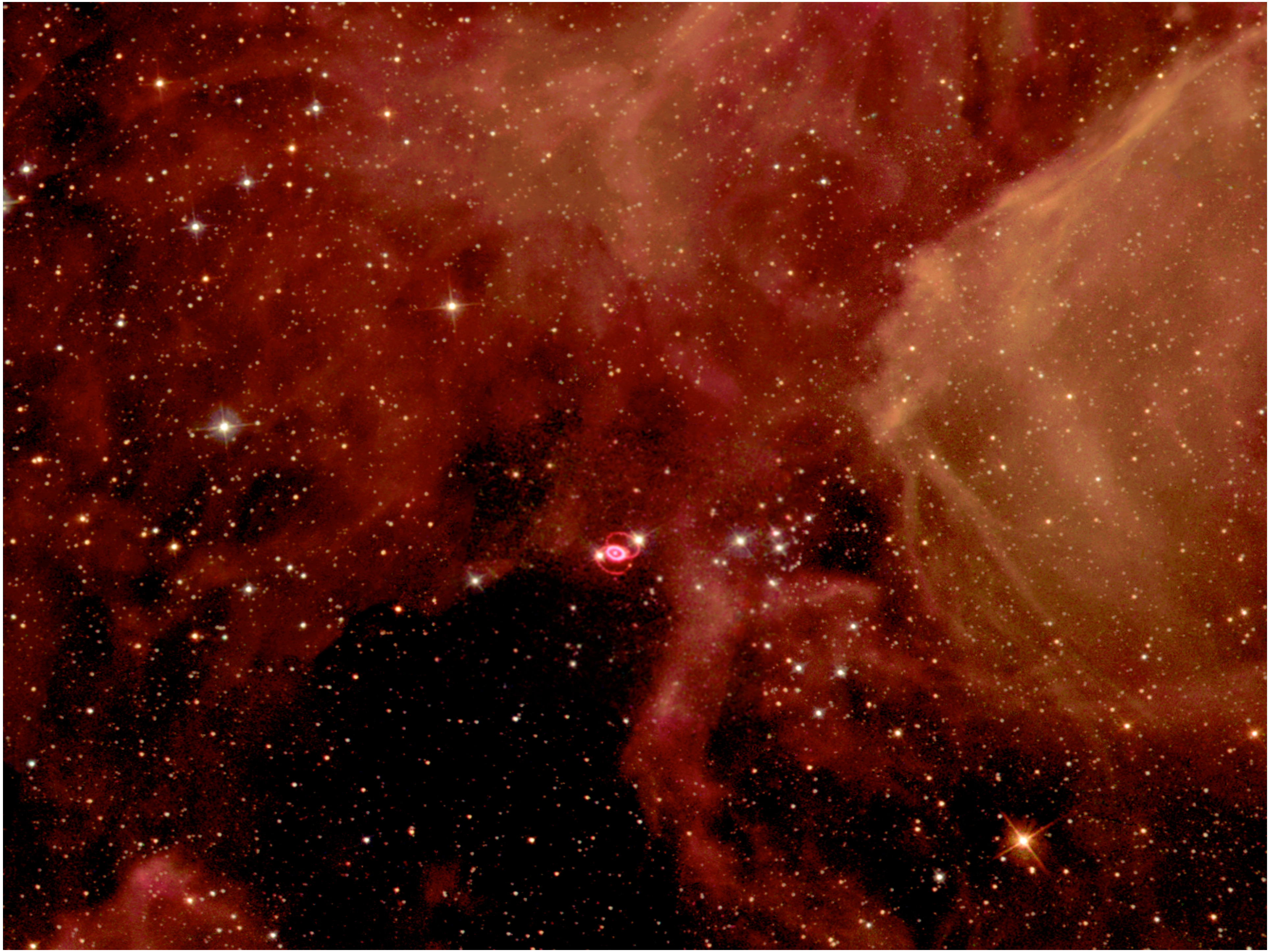

SUPERNOVAE

- 1934 - Baade (gravitation energyof SN : neurtron star + envelope of SN)
- 1960- Fowler (Nobel Prize),Hoyle (1-thermal instability; 2 - collapse)
- 1966-Colgate, White (numerical model: collapse□ neutrino emission □ throw out the envelope □ neurtron star)
- 1966-67-Arnett (numerical model of detonation supernova)
- 1970-Imshennik, Nadezin(neutrino diffusion- t about 10 sec.)
- 1974-Chechetkin,Imshennik,Ivanova(deflagration model of SN, in 1997 model of nucleosynthesis □ formation of elementsin “Fe”-peak and formation of heavy elementsin Chechetkin,Ptisin 1980-_)

The decay of the detonation wave of burning in degenerate CO cores of supernovae.

Imshennik V.S., Kal'yanova N.L., Koldoba A.V., Chechetkin V.M. Astronomy Letters, Vol.25, No 4, 1999, pp.206-214.

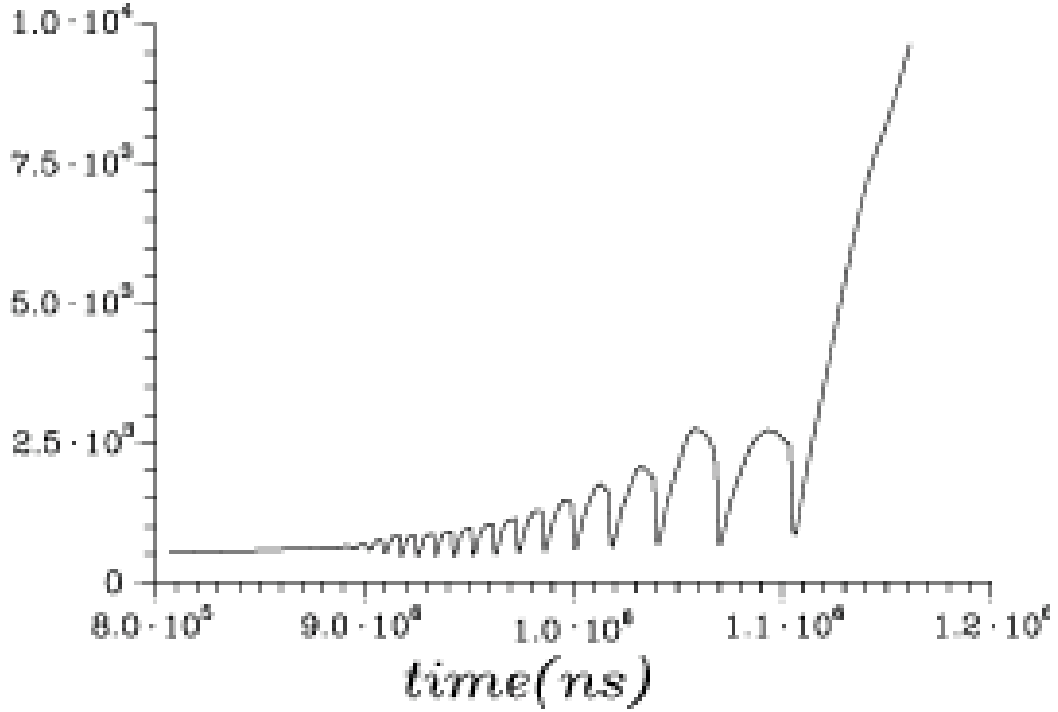

a) The width of the reaction zone [cm] of the shock wave as a function of time.

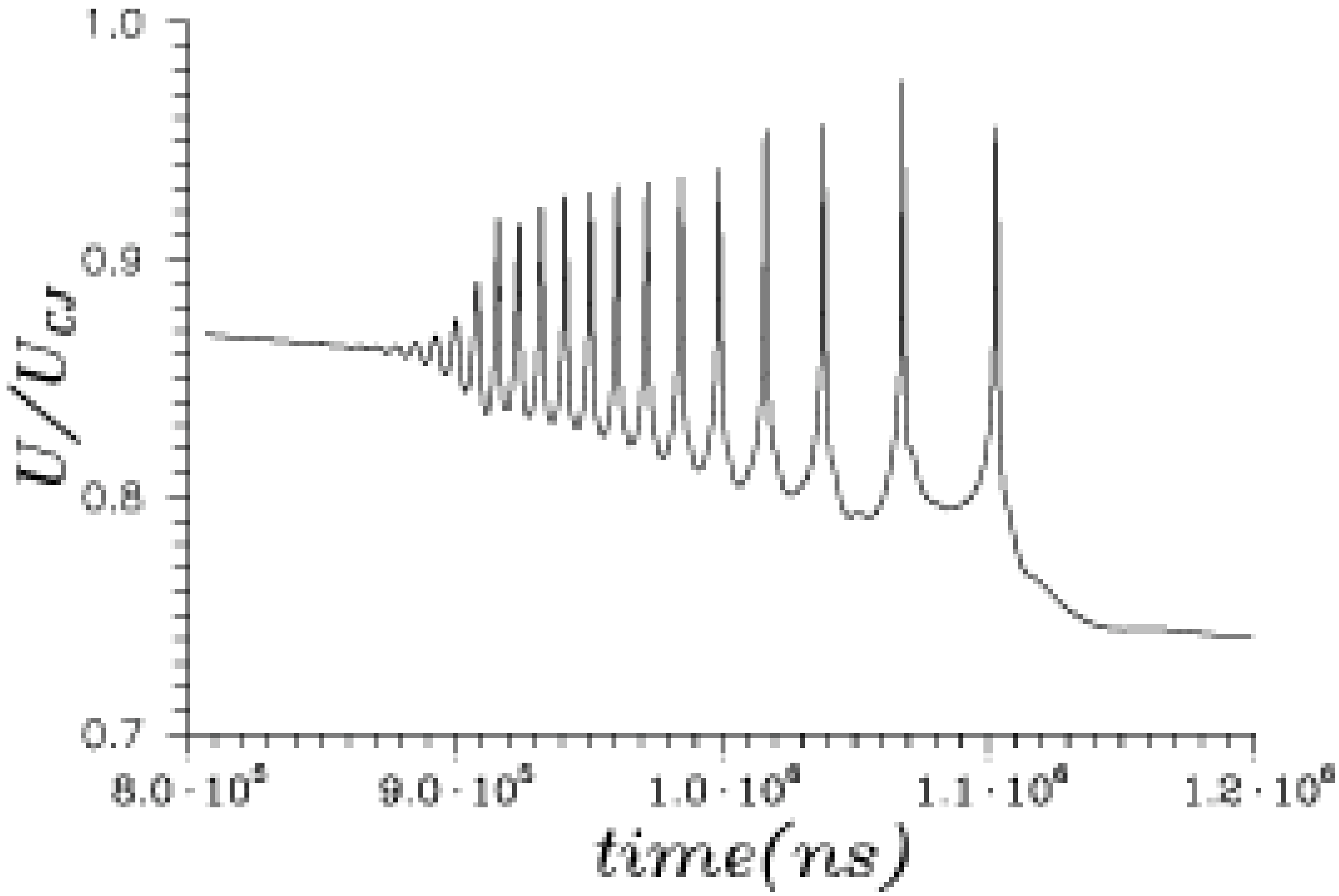

b) The degree of deceleration f=U/Ucj of the shock wave as a function of time.

Entropy T=0.68 s

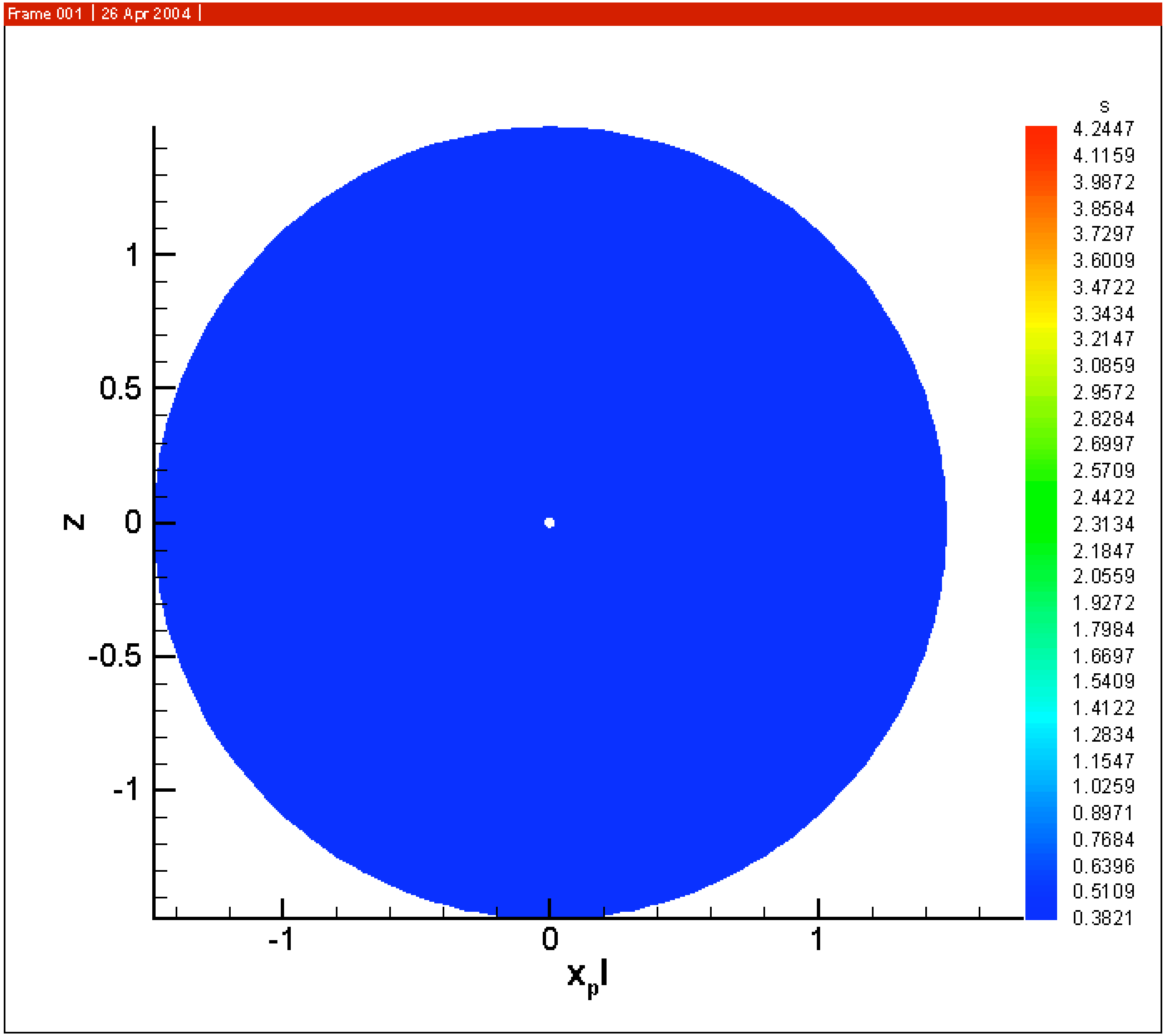

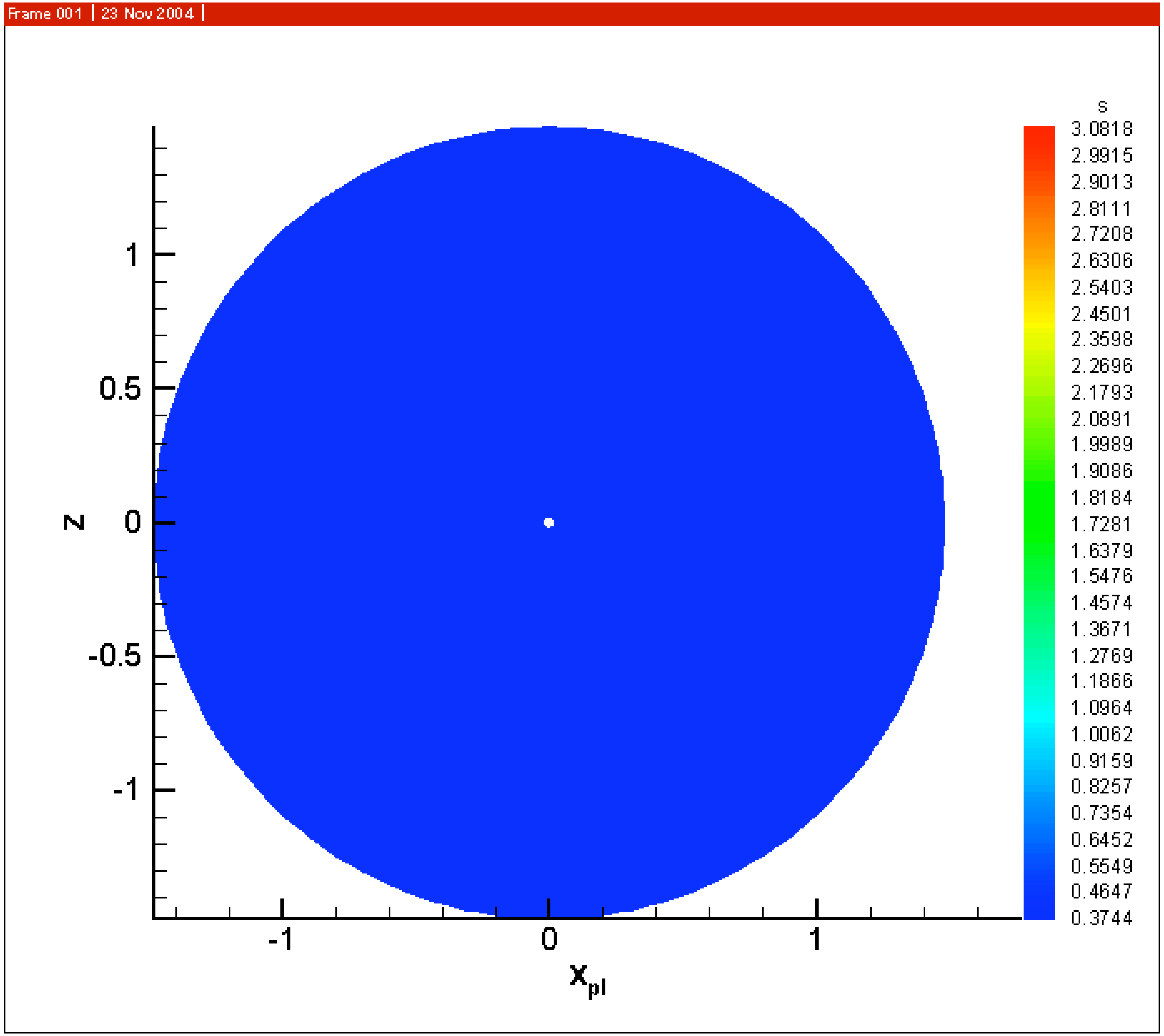

Frame 001 | 23 Nov 2004 |
s
3.0818
2.9915
2.9013
2.8111
2.7208
2.6306
2.5403
2.4501
2.3598
2.2696
2.1793
2.0891
1.9989
1.9086
1.8184
1.7281
1.6379
1.5476
1.4574
1.3671
1.2769
1.1866
1.0964
1.0062
0.9159
0.8257
0.7354
0.6452
0.5549
0.4647
0.3744
z
1
0.5
0
-0.5
-1
-1
0
1
x_{pl}

Supernovae (continuation)

- **1980- Chechetkin, Gershtein, Imshennik, Khlopov(neutrino ignition in SN model***
- **1981-Chechetkin, Ivanova ("Fe"-core with 1 _⊙ , energy of SN is equal 5 10↑50 erg)***
- **1990- Cooperstein, Baron ("Fe"-core with 1.1 _⊙, energy of SN is equal 10↑51 erg, for massive stars the explosion of SN is absent, model «prompt shock»)**
- **1986-1989 - Chechetkin, Popov (the explosionof therotatihg __-core throw out of envelope along rotating axis - jets)**
- **1989-Colgate _ Wilson,Mayle(model «delay shock» -energy of SN 10↑48 erg)**
- **1994-1996 -Chechetkin (large-scale instability in SN II expplosion)**
- **1963- Chandrasekhar,Lebovitz,Ap.J.p138**
- **2004 – Chechetkin, Popov, Ustuygov (large-scale instability in SN I expplosion), Astr. Rep., 2004, vol. 10, p.1-14.**

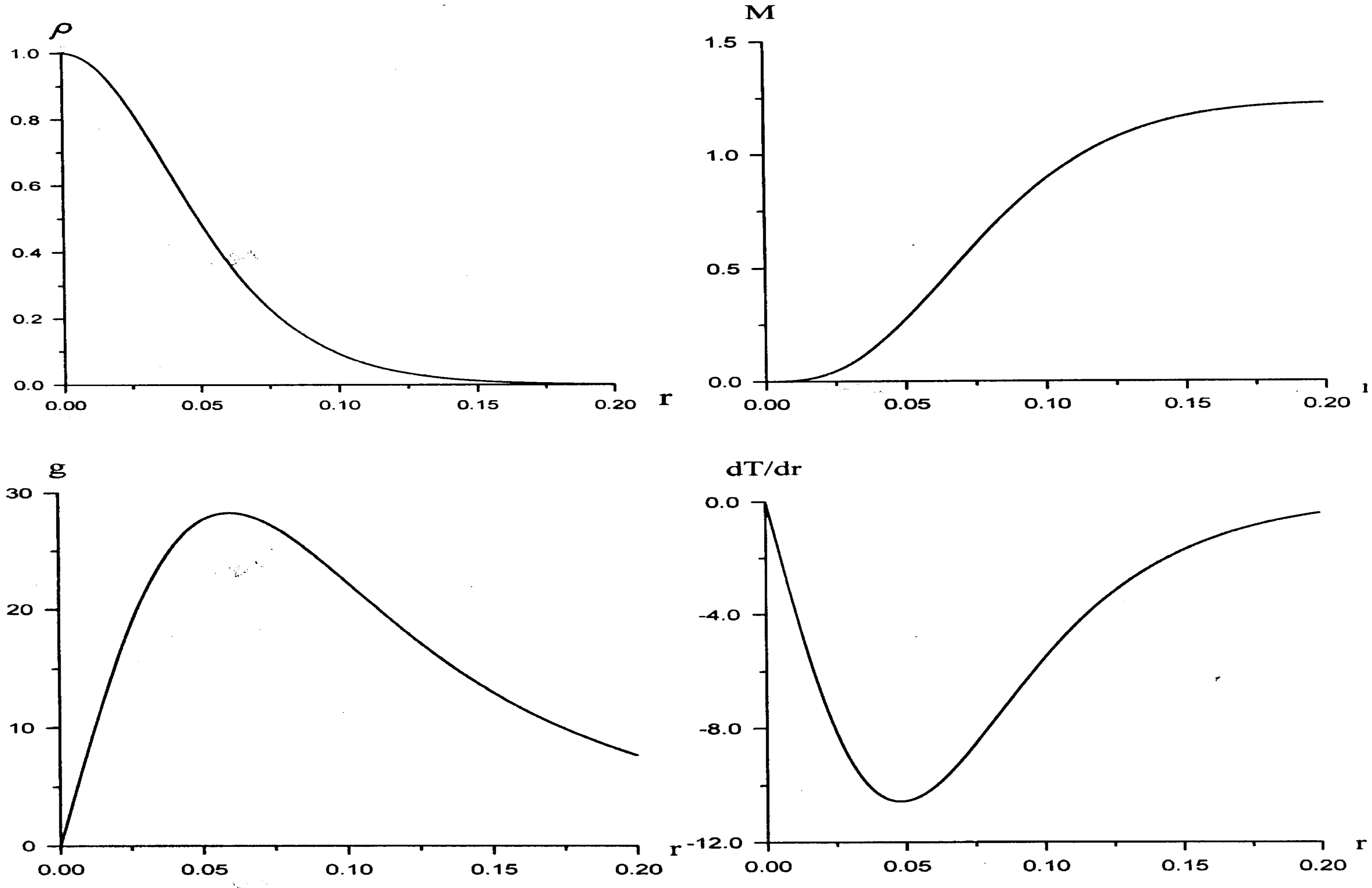

ρ
1.0
0.8
0.6
0.4
0.2
0.0
0.00
0.05
0.10
0.15
0.20
r
M
1.5
1.0
0.5
0.0
0.00
0.05
0.10
0.15
0.20
g
30
20
10
0
0.00
0.05
0.10
0.15
0.20
r
dT/dr
0.0
-4.0
-8.0
-12.0
0.00
0.05
0.10
0.15
0.20
r

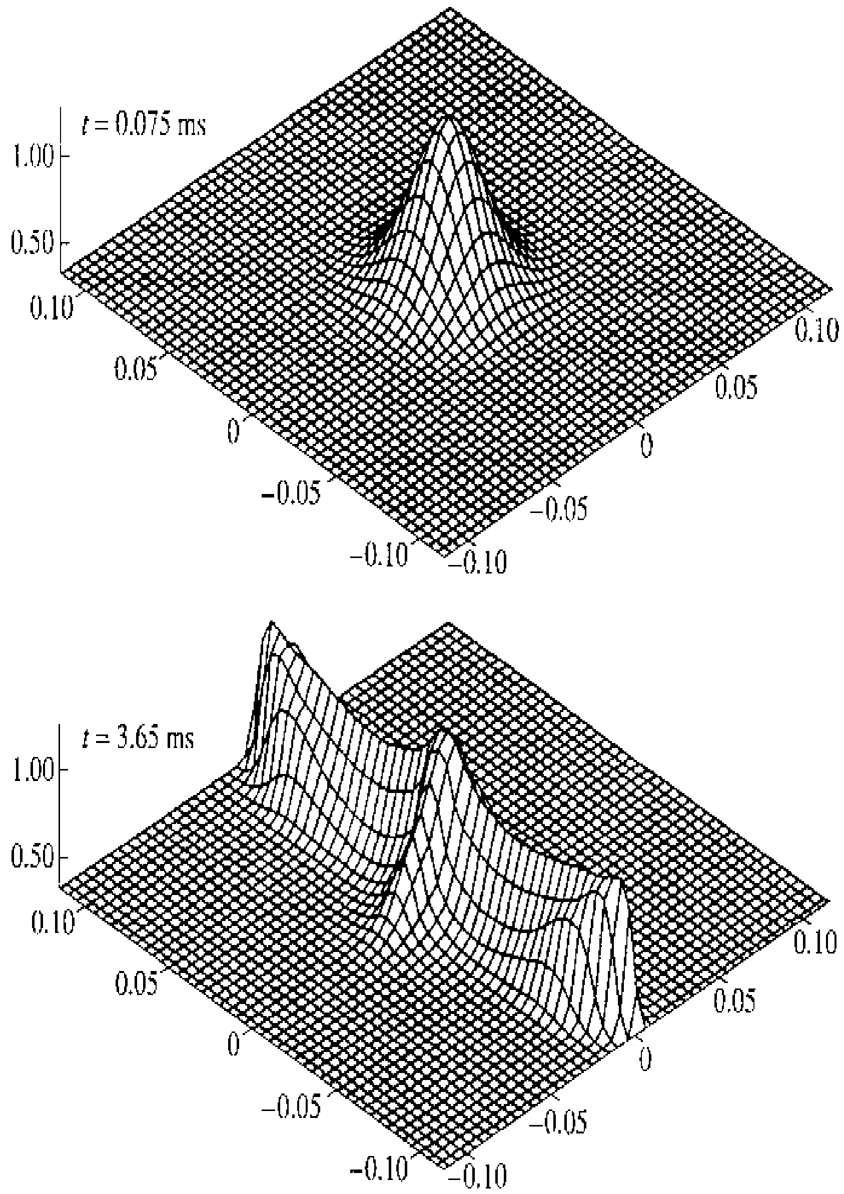

Fig. 3. Three-dimensional entropy profile for two characteristic times. The axis scales are the same as in Fig. 1.

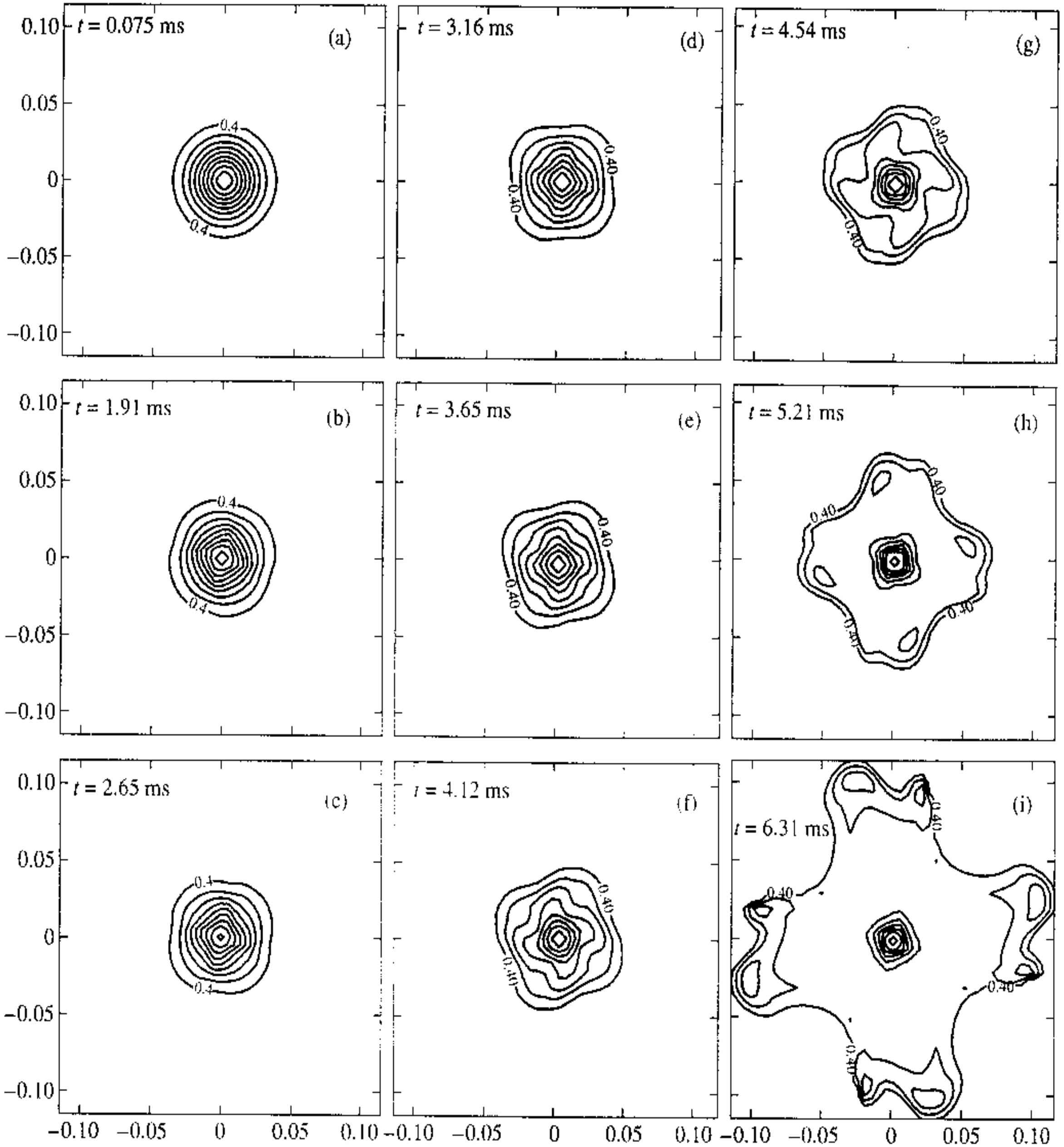

Fig. 2. Same as for Fig. 1, but in the equatorial plane.

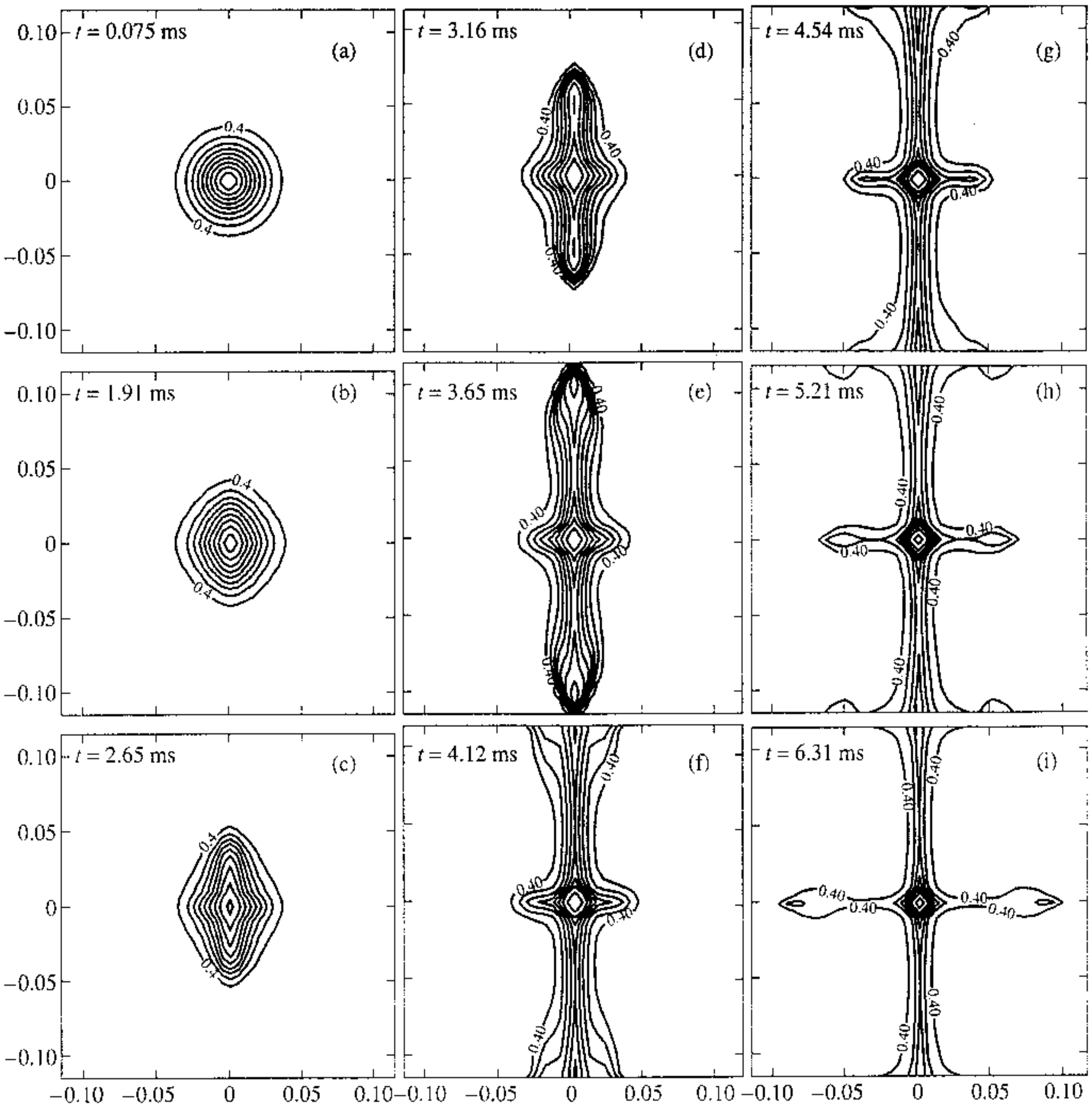

Fig. 1. Levels of constant entropy in the Ozx plane. Both axes have scales in fractions of the characteristic length; 0.1 corresponds to 20 km. The entropy is expressed in dimensionless units, normalized to the Boltzmann constant and the nucleon density. The initial background entropy is 1.6327 k_B/nucl (corresponding to the normalized value 0.37).

Rigid body rotation. $E_{rotation} = 0.01\ E_{binding\ gravitation}$

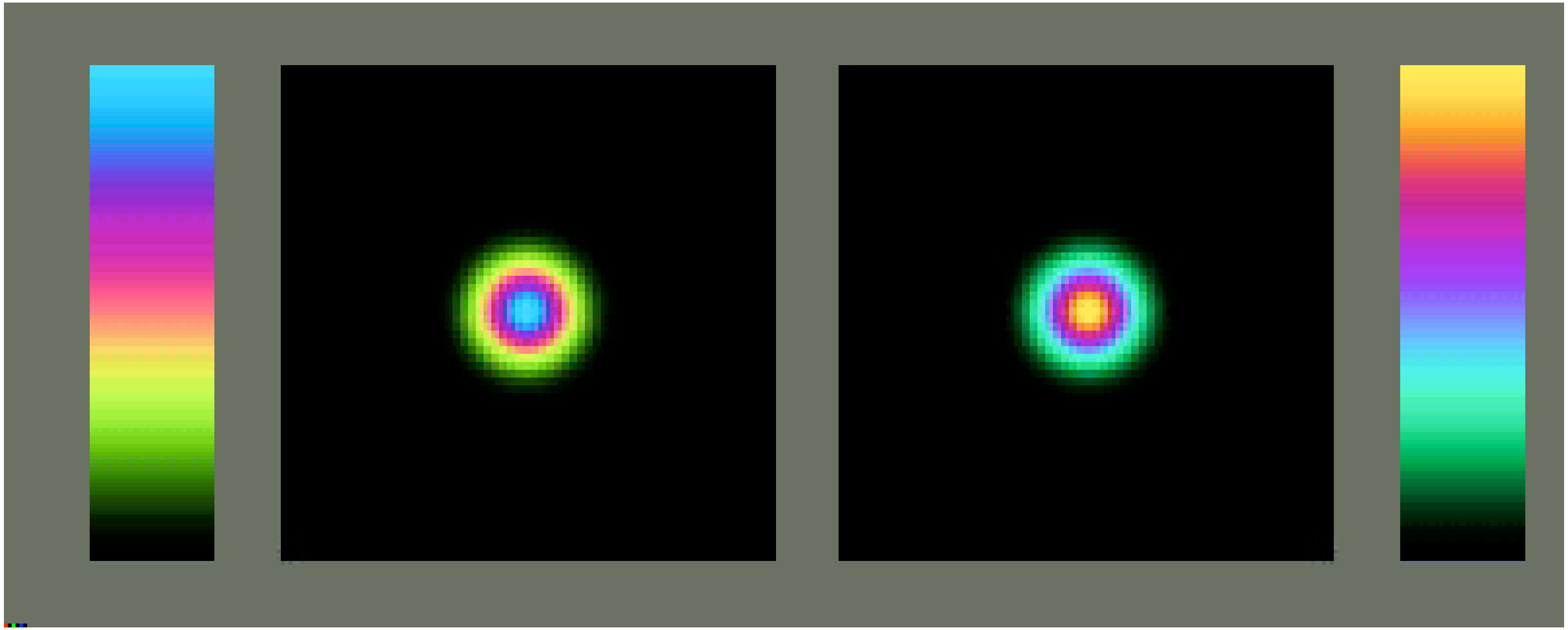

Rigid body rotation. $E_{rotation} = 0.05\ E_{binding\ gravitation}$

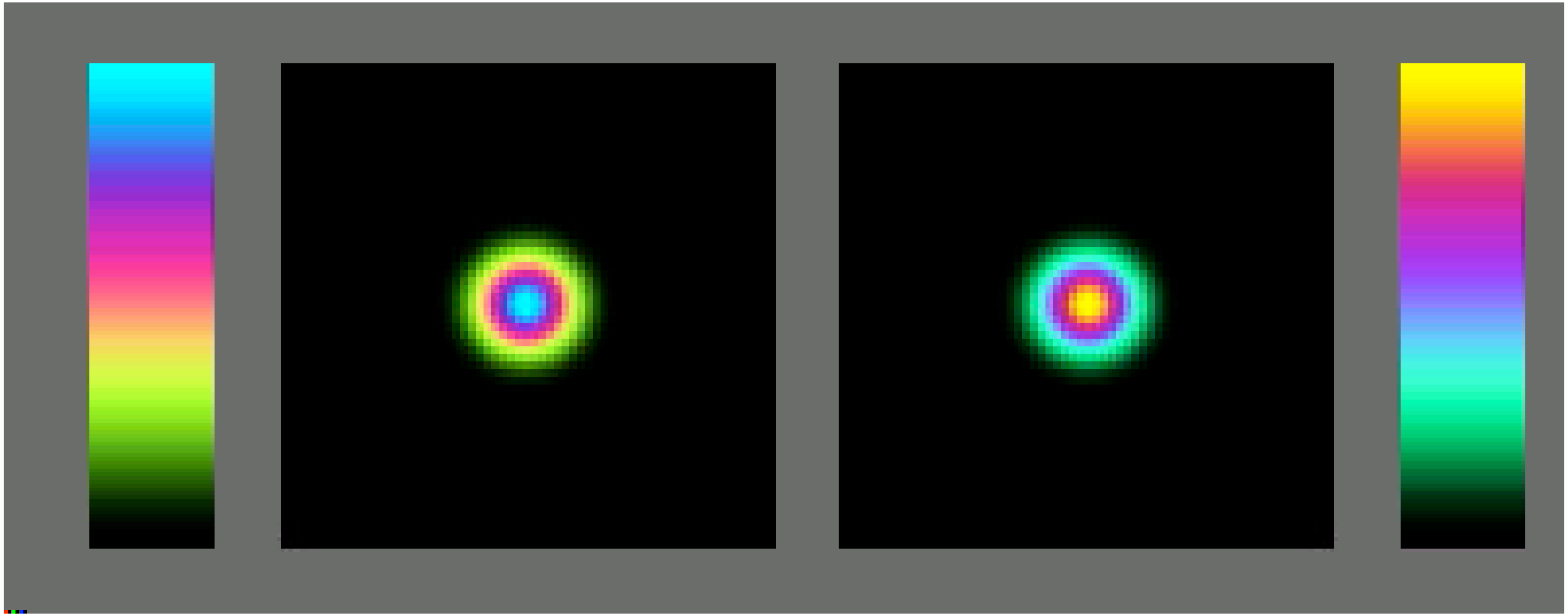

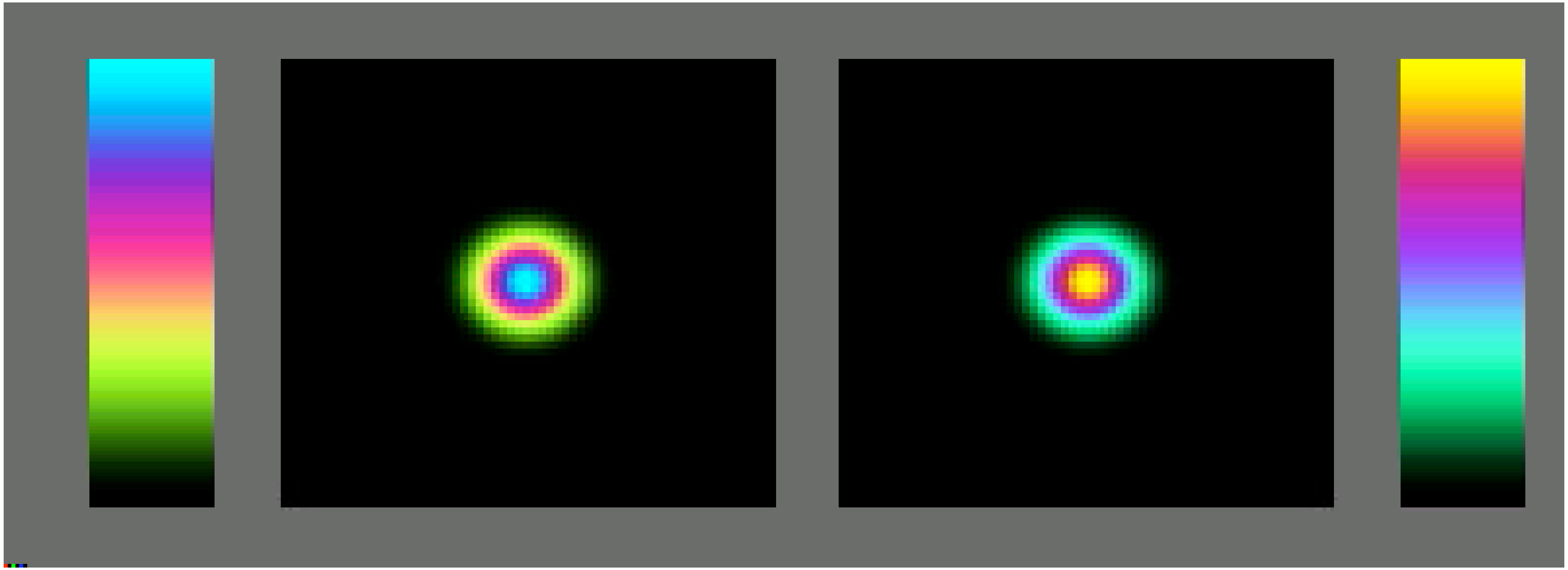

Differential rotation. $E_{rotation} = 0.05\ E_{binding\ gravitation}$

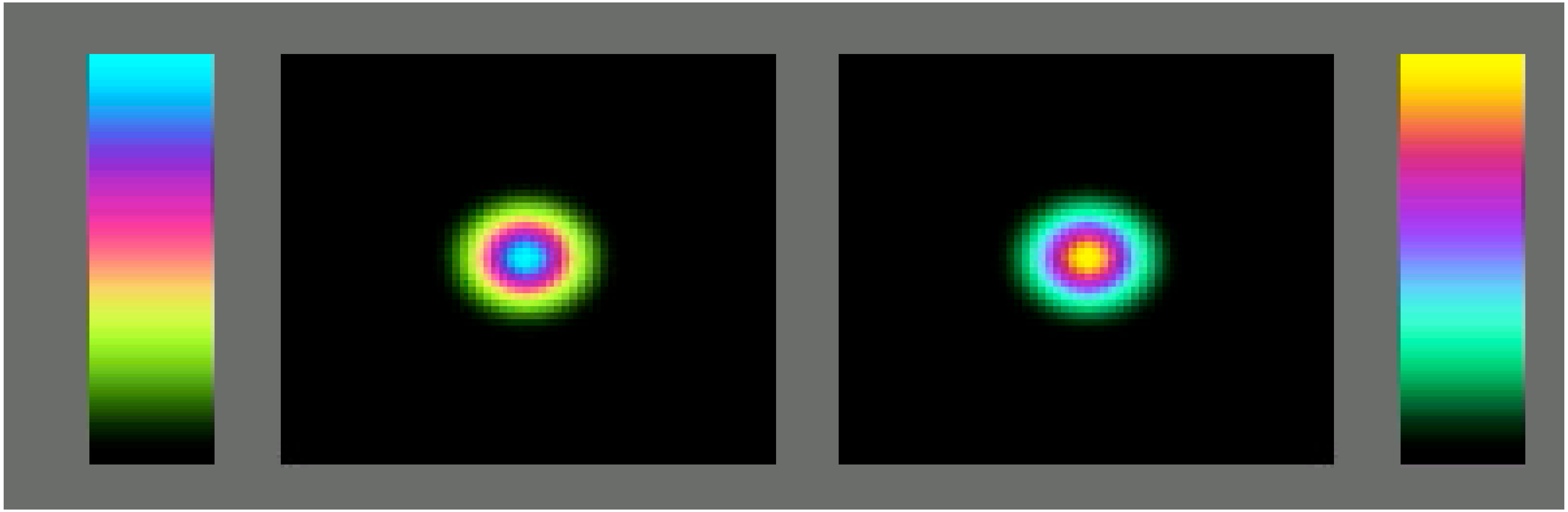

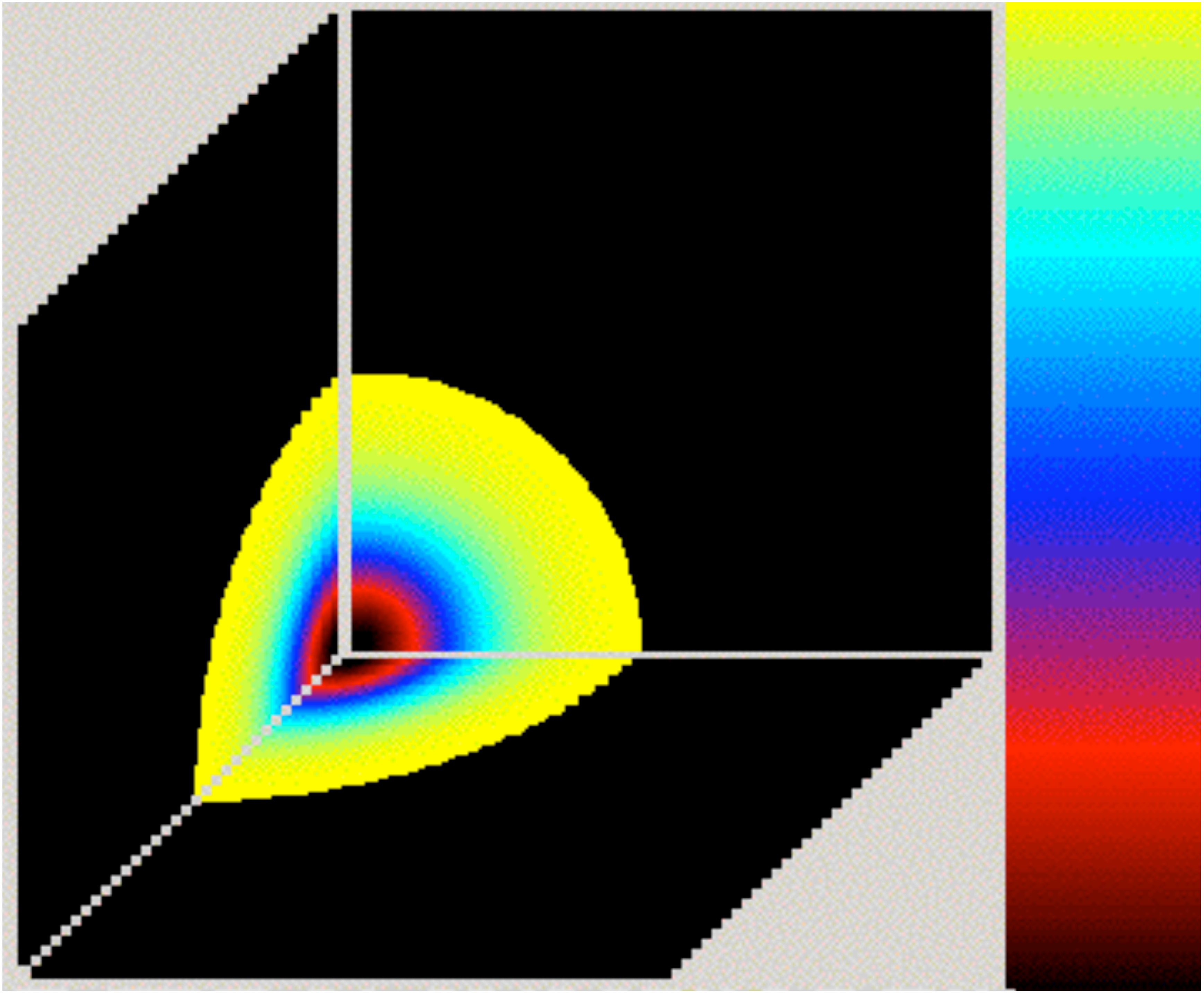

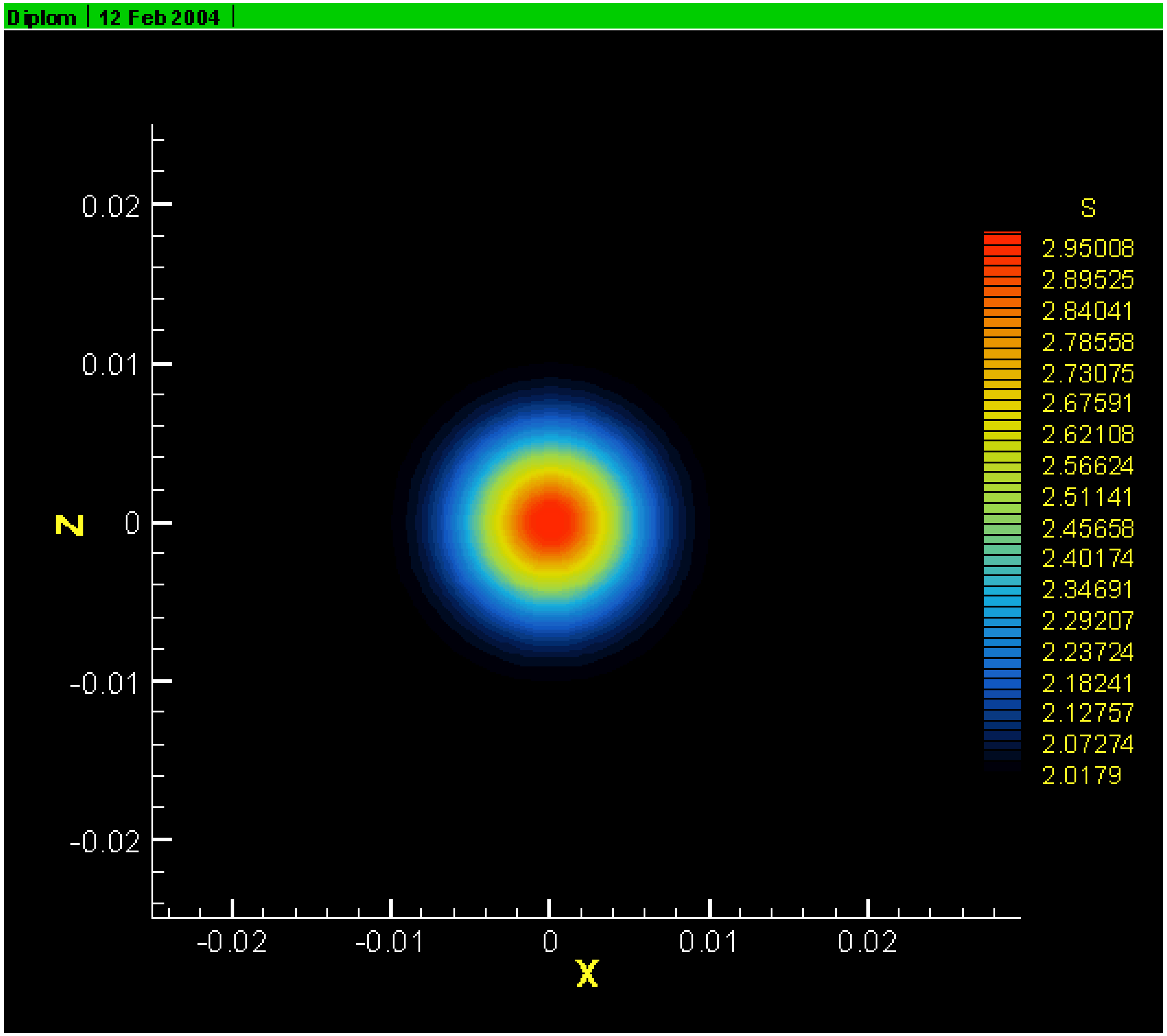
Diplom | 12 Feb 2004 |
0.02
0.01
Z
0
-0.01
-0.02
-0.02
-0.01
0
0.01
0.02
X
S
2.95008
2.89525
2.84041
2.78558
2.73075
2.67591
2.62108
2.56624
2.51141
2.45658
2.40174
2.34691
2.29207
2.23724
2.18241
2.12757
2.07274
2.0179

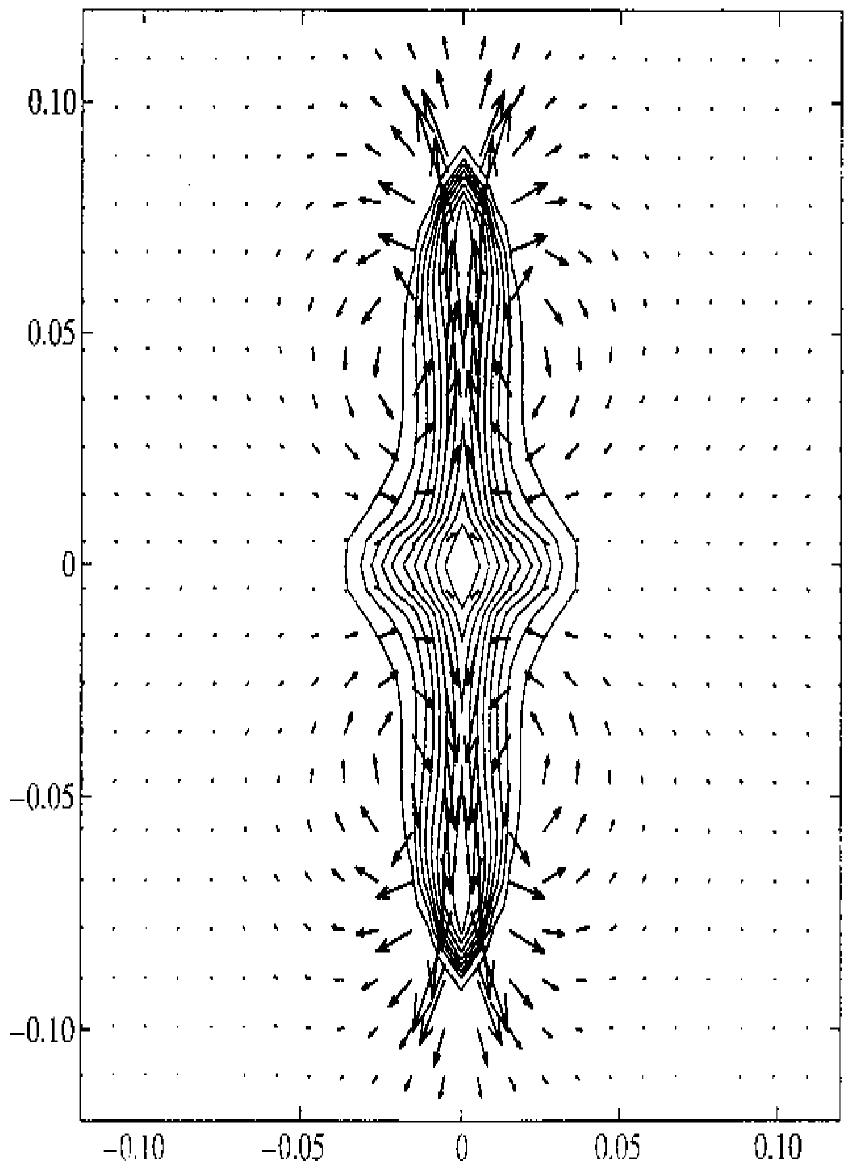

Fig. 4. Distributions of the entropy and velocity field in the Ozx plane during the formation and initial motion of a bubble toward the neutrinosphere. The axis scales are the same as in Fig. 1.

inside the region. The mean bubble density was determined by averaging over all computational cells inside the bubble. Since we are primarily interested in relatively rough estimates, we shall consider a model that describes the matter in the perturbed region and relevant neutrino processes only approximately, but retains the features we consider to be most important.

To simplify the model, we assume that, at the initial time, the bubble is composed of iron nuclei ($A = 56$, $Z = 26$) and free ultrarelativistic electrons. At densities of 2×10^{14} g/cm^3, such a medium is characterized by intense beta processes, which are a source of neutrinos:

$$(A, Z) + e \Rightarrow (A, Z-1) + \nu.$$

Inverse processes that absorb neutrinos also occur:

$$(A, Z+1) + e \Leftarrow (A, Z) + \nu.$$

Both direct and inverse beta processes produce new elements, complicating the model for the medium. To avoid this, we introduce a neutron component and do not distinguish between different types of nuclei. Along with inelastic processes, neutrinos also participate in elastic interactions with electrons and nuclei:

$$(A, Z) + \nu \Rightarrow (A, Z)' + \nu',$$

$$e + \nu \Rightarrow e' + \nu'.$$

We emphasize that, due to the large difference between the masses of electrons and nuclei, neutrinos lose substantially greater energy in collisions with electrons. Since our treatment will be limited to a uniform and isotropic approximation for the neutrino distribution function (whereas scattering by nuclei contributes appreciably only to the anisotropic component of the distribution function), we can neglect scattering by nuclei in the collision integral. However, since scattering by nuclei appreciably affects the rate of escape of neutrinos through the bubble boundary, we will taken it into account in this process. We neglect all other processes involving neutrinos. In contrast to [5], we shall take into account the fact that there is also some distribution of neutrinos outside the bubble. Therefore, neutrinos can both leave and enter the region under consideration. The electron distribution function will be interpolated by a Fermi step function, which is obviously applicable only when $E_F \gg 1.5kT$ (i.e., when the Fermi energy of the electrons is considerably greater than their thermal energy).

3. THE MATHEMATICAL MODEL

In a uniform, isotropic approximation, the kinetic equation describing the evolution of the neutrino distribution in a bounded region whose characteristic size d, density, and partial concentrations of components vary with time can be written in the form

$$\begin{aligned}\frac{\partial f(p,t)}{\partial t} &= 4\pi\Big[(1-f(p,t))\int_0^\infty dp'(p')^2 \\ &\quad\times f(p',t)K^{\mathrm{in}}(p,p',t) \\ &\quad - f(p,t)\int_0^\infty dp'(p')^2(1-f(p',t))K^{\mathrm{out}}(p,p',t)\Big] \\ &\quad + \frac{d\rho(t)}{\rho(t)dt}f(p,t) + (1-f(p,t))S(p,t) \\ &\quad - f(p,t)Y(p,t) - \frac{c}{d(t)[1+\gamma(p,t)]}(f(p,t)-f_g(p,p_g)).\end{aligned} \quad (1)$$

Here, the functions $K^{\mathrm{in}}(p, p' t)$ and $K^{\mathrm{out}}(p, p', t)$ depend on details of the process of neutrino scattering by electrons, and $S(p, t)$ and $Y(p, t)$ are sources and sinks of neutrinos, determined by the direct and inverse beta processes. The term containing the logarithmic derivative of the density is responsible for variations in the neutrino distribution due to the changing dimensions of the region where the neutrinos are concentrated. The last term describes neutrino escape through the boundary. (The value $\gamma = 0$ corresponds to the case of free propagation.) We normalized the distribution function as follows:

$$n(t) = 4\pi(2\pi\hbar)^{-3}\int_0^\infty dp'(p')^2 f(p',t). \quad (2)$$

This equation for the neutrino distribution function must be supplemented by an equation describing evolution of the electron number density

$$\begin{aligned}\frac{dn_e(t)}{dt} &= 4\pi\int_0^\infty dp p^2 \\ &\quad\times[-(1-f(p,t))S(p,t) + f(p,t)Y(p,t)] + \frac{d\rho}{\rho dt}n_e(t),\end{aligned} \quad (3)$$

and also by a relation between the densities of the electrons and neutrons, on the one hand, and the density of the medium, on the other:

$$m_n\Big[n_n(t) + \frac{A}{Z}n_e(t)\Big] = \rho(t). \quad (4)$$

In deriving (4), we have assumed that electrons make a negligible contribution to the density of the medium, and that the medium is electrically neutral.

To facilitate use of the above equations as a basis for numerical simulations, we introduce dimensionless variables, constructed using the following parameters: characteristic length 3×10^7 cm, characteristic time 10^{-3} s, characteristic density 2×10^{14} g/cm^3, characteristic momentum $p_F(0) = s^{-1} E_F(0)$ (the Fermi-momentum of the electrons, where $E_F(0) = 219$ MeV), and characteristic number density of the particles $n_e(0) = 4.63 \times 10^{37}$ cm^{-3}. The dimensionless characteristic size $d(t)$ at the initial time is $d(0) = 2.13 \times 10^{-2}$.

We shall not introduce special notation for the dimensionless quantities (apart from $p \longrightarrow x, p' \longrightarrow y$, and $P_F \longrightarrow u$). The required dimensionless system of equations will then take the form

$$\frac{df(x,t)}{\partial t} = 4\pi[(1-f(x,t))\int_0^{\infty} dy y^2 f(y,t) K^{\text{in}}(x,y,t)$$

$$-f(x,t)\int_0^{\infty} dy y^2 (1-f(y,t)) K^{\text{out}}(x,y,t)]$$

$$+\frac{d\rho}{\rho dt} f(x,t) + (1-f(x,t)) S(x,t) \tag{5}$$

$$-f(x,t)Y(x,t) - \frac{1}{d(1+\gamma)}(f(x,t) - f_g(x,x_g)),$$

$$\frac{dn_e(t)}{dt} = \frac{3}{2}\int_0^{\infty} dx x^2$$

$$\times[-(1-f(x,t))S(x,t) + f(x,t)Y(x,t)] + \frac{d\rho}{\rho dt} n_e(t), \tag{6}$$

$$n_n(t) + \frac{A}{Z} n_e(t) = \frac{A}{Z}\rho(t). \tag{7}$$

The time dependence of the characteristic size d is given by the expression

$$d(t) = d(0)\sqrt[3]{\frac{\rho(0)}{\rho(t)}}. \tag{8}$$

The normalization of the neutrino distribution function becomes

$$n(t) = \frac{3}{2}\int_0^{\infty} dx x^2 f(x,t). \tag{9}$$

Formulas for $S(x, t)$ and $Y(x, t)$ are presented in [6]. We shall write here only the corresponding dimensionless relations:

$$S(x,t) = 1.874 \times 10^3 \left(\frac{Z}{A}\rho(0)\right)^{5/3}$$

$$\times x^2 \theta(u(t) - x)\frac{n_e(t)}{Z}, \tag{10}$$

$$Y(x,t) = 1.874 \times 10^3 \left(\frac{Z}{A}\rho(0)\right)^{5/3} x^2 \theta(x - u(t))$$

$$\times\left[\frac{n_e(t)}{Z} + 100\frac{A}{Z}\left(\frac{\rho(t)}{\rho(0)} - n_e(t)\right)\right]. \tag{11}$$

(In addition, the relation $n_e(t) = u^3(t)$ is valid in the dimensionless notation.)

We used the following expressions for γ in the simulations:

$$\gamma(x,t) = 4\pi\int_0^{\infty} dy y^2 (1 - f(y,t))$$

$$\times[K^{\text{out}}(x,y,t) + K^n(x,y,t)], \tag{12}$$

and

$$\gamma(x,t) = 4\pi\int_0^{\infty} dy y^2$$

$$\times[(1-f(y,t))K^{\text{out}}(x,y,t) + K^n(x,y,t)]. \tag{13}$$

The function $K^n(x, y, t)$ describes scattering by nuclei:

$$K^n(x,y,t) = 1.69 \times 10^6 \left(\frac{A}{10}\right)^2$$

$$\times\left(\frac{Z}{A}\rho(0)\right)^{5/3}\frac{n_e(t)}{z}\delta(x-y),$$

$$K^{\text{in/out}}(x,y,t) = 2.326 \times 10^6 (xy)^{-2} \tag{14}$$

$$\times\left(\frac{Z}{A}\rho(0)\right)^{5/3} r^{\text{in/out}}(x,y,t).$$

Let us write also the quantities $r(x, y, t) = r(x, y, u(t))$, taken from [6]:

(1) For $0 \le x \le u(t)$:

$$r^{\text{out}}(x,y,u) = \theta(x-y)y^3\left[\frac{8}{9}((u+x)^3 - u^3)\right.$$

$$\left.-y\left(2x^2 + 4ux + \frac{8}{3}u^2\right) + y^2\left(\frac{8}{5}x + \frac{4}{3}u\right) - \frac{22}{45}y^3\right], \tag{15}$$

$$r^{\text{in}}(x,y,u) = x^3\theta(u-y)\theta(y-x)$$

$$\times\left[\frac{8}{9}y^3 + \frac{2}{3}(4u - 3x)y^2 + \left(\frac{8}{5}x^2 - 4ux + \frac{8}{3}u^2\right)y\right.$$

$$\left.+\left(-\frac{22}{45}x^3 + \frac{4}{3}ux^2 - \frac{8}{3}u^2 x\right)\right] + x^3(u-x)\theta(y-u)$$

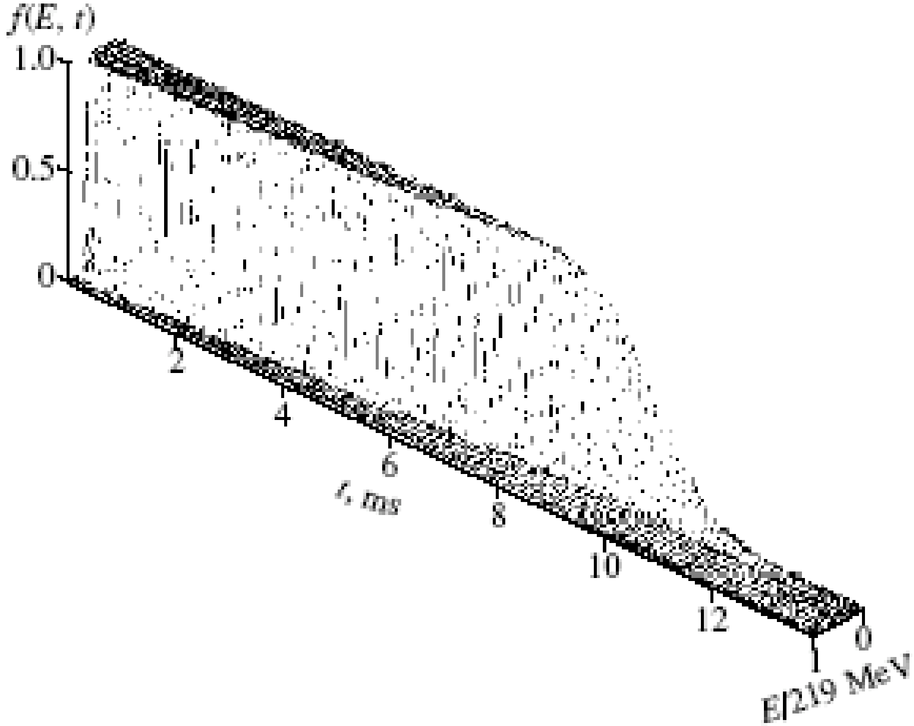

Fig. 3. Neutrino distribution function $f(E, t)$.

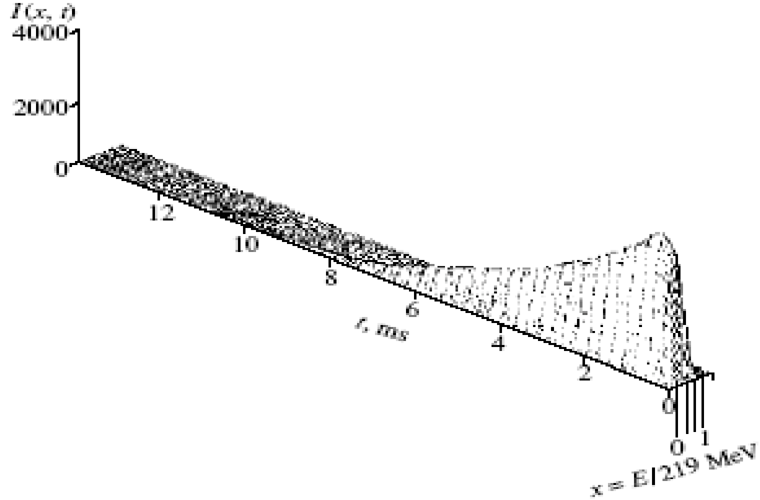

Fig. 4. The function $I(x, t)$.

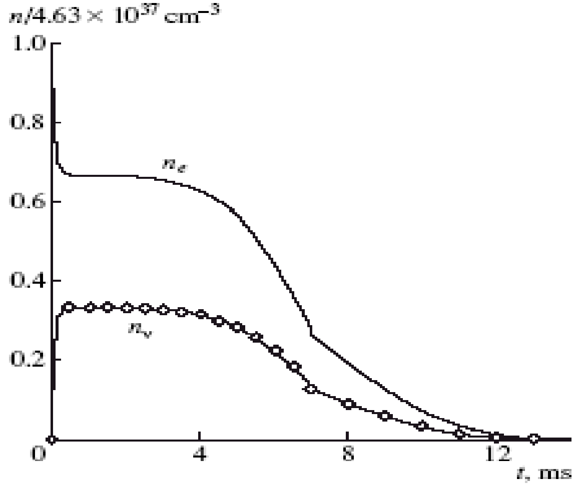

Fig. 5. Time dependence of the number density of neutrinos (marked curve) and electrons (unmarked curve).

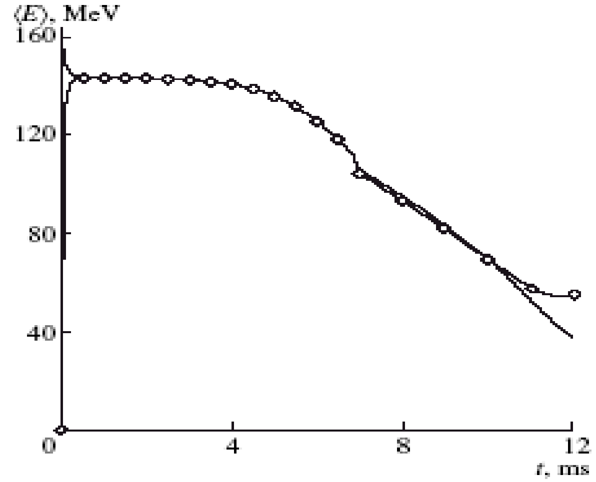

Fig. 6. Time dependence of the average energies of the neutrinos (marked curve) and electrons (unmarked curve).

cesses) to $t \approx 10$ ms (when the medium becomes optically thin). In the first case (Fig. 2), the average neutrino energy is less than the average electron energy, due to the emission of some of the neutrinos before the onset of the stage of "classical" transparency. Later, the mean neutrino energy exceeds the mean electron energy in both cases, since the degradation of neutrinos in νe processes is substantially decreased, while the Fermi energy of the electrons (and, consequently, their average energy) continues to decrease as the bubble expands.

In conclusion, let us estimate the spectrum of the neutrinos emitted from a supernova in the adopted scenario. In the second case, the spectra of the neutrino emission from the bubble and from the entire supernova should coincide to high accuracy, since the bubble radiation is emitted in the optically thin region of the

Simulation of Neutrino Transport by Large-Scale Convective Instability in a Proto-Neutron Star

(Suslin, Ustyugov, Chechetkin, Churkina, 2000, Ast.Rep., V 45, March 2001)

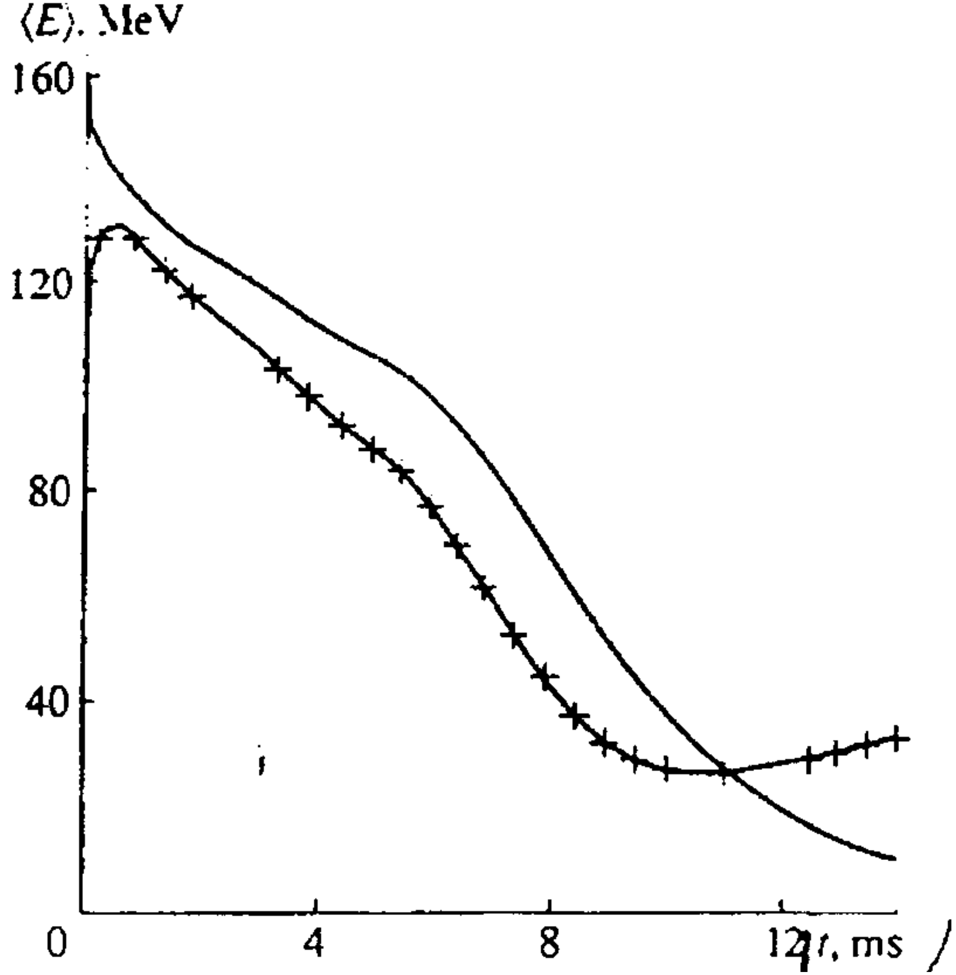

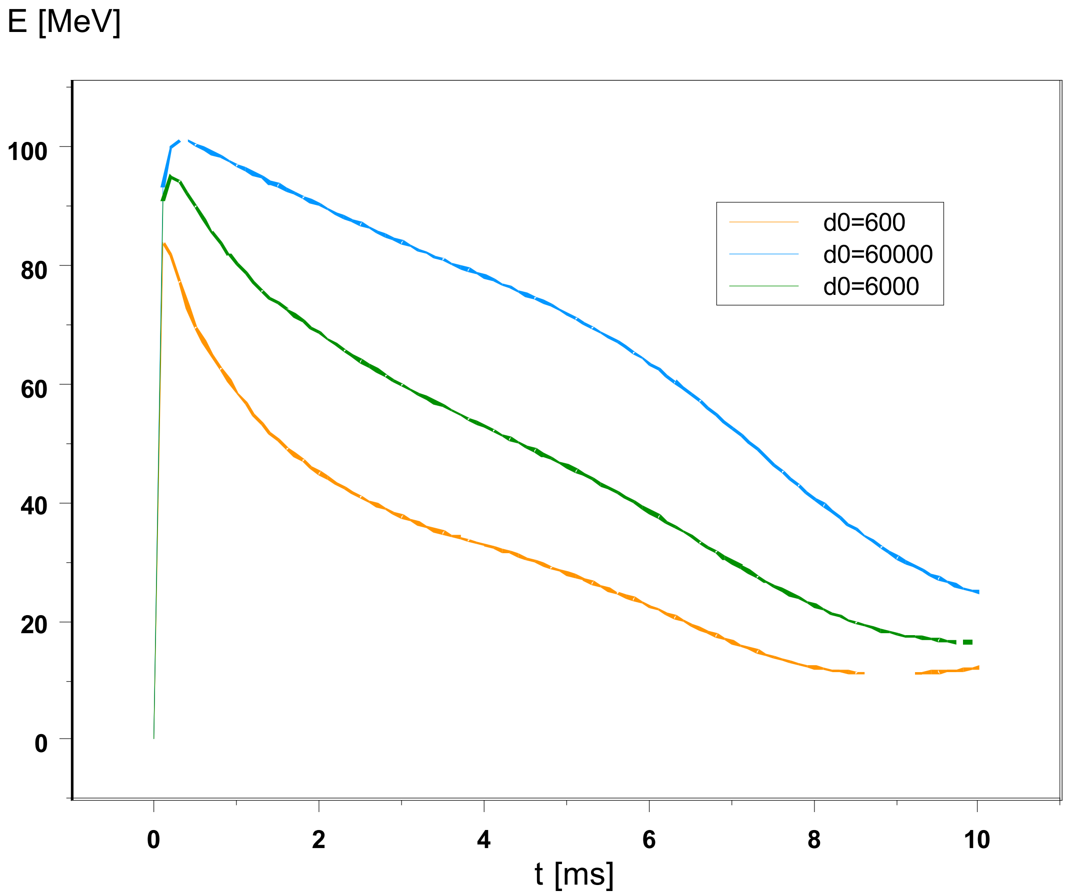

E [MeV]
100
80
60
40
20
0
0
2
4
6
8
10
t [ms]
d0=600
d0=60000
d0=6000

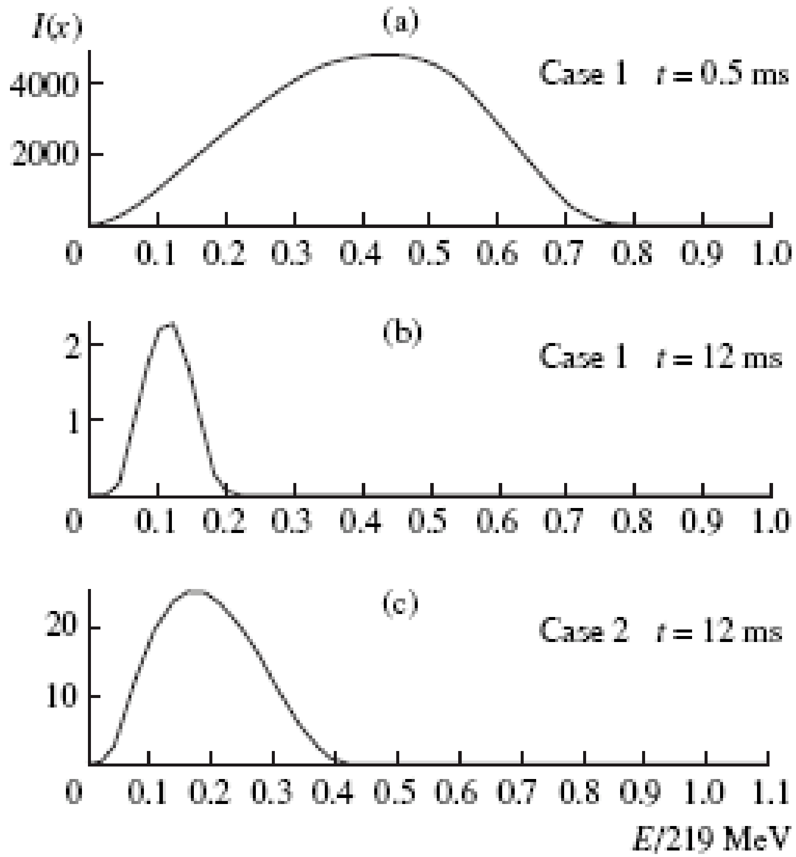

Fig. 8. Spectra of the emitted neutrinos $I(x)$.

In work (Baikov I. V. and Chechetkin V. M., Astron.Rep., 2004, in press) has been kinetic energy of outflow envelope of supernova II type in the depend of mean neutrino energy which must emit from protoneutron star. This energy increase when mean neutrino energy increase too. For example then neutrino energy at 2 time (from 30 MeV to 60 MeV) then kinetic energy of envelope increase on the 20%. Then mean neutrino energy is near 5 MeV the effect outflow is small.

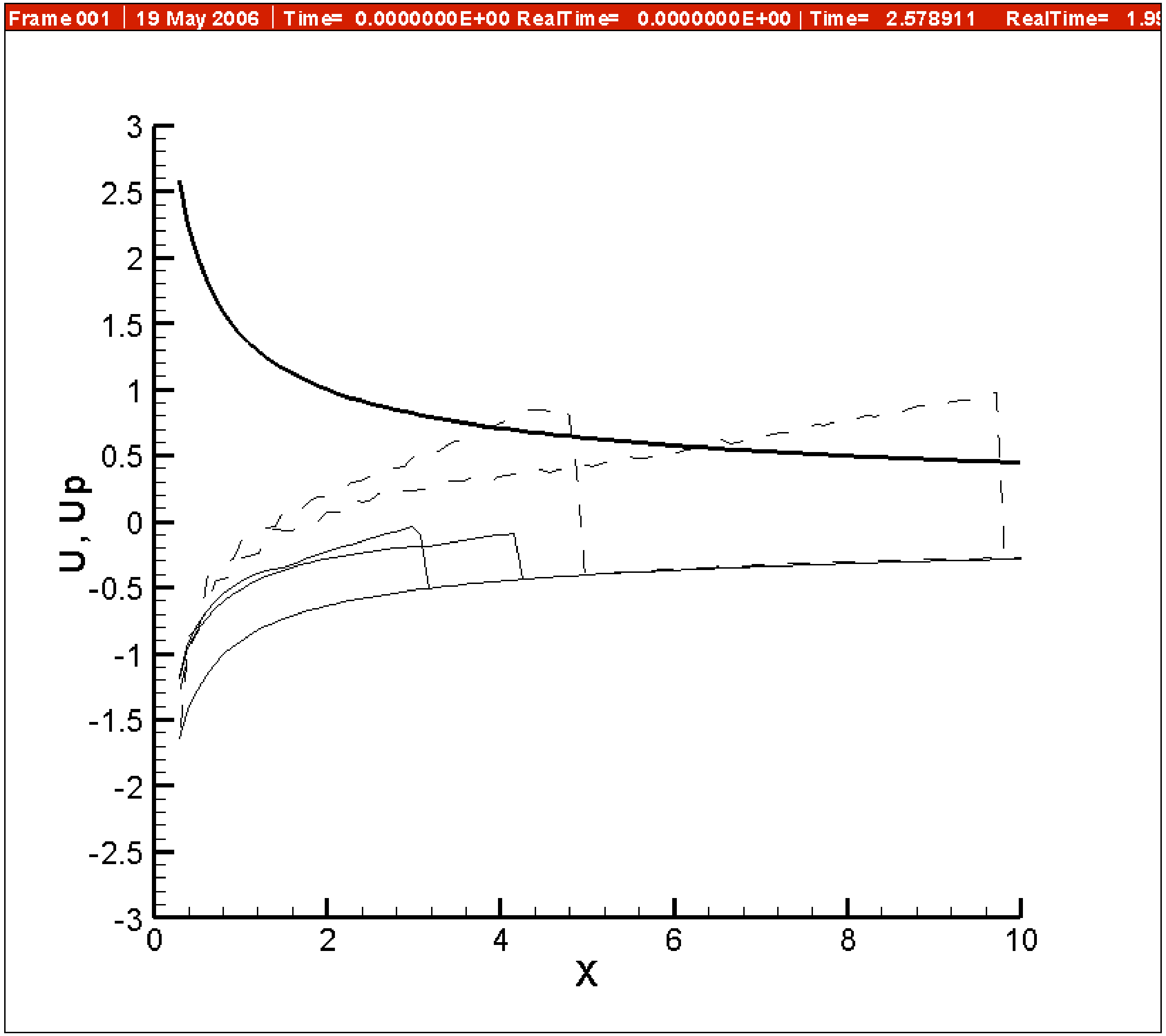

$$\square(r) = \frac{\dot{M}}{4\square}\frac{r^{3/2}}{v_0\sqrt{GM}}, \quad v(r) = \square v_0\sqrt{\frac{GM}{r}}$$

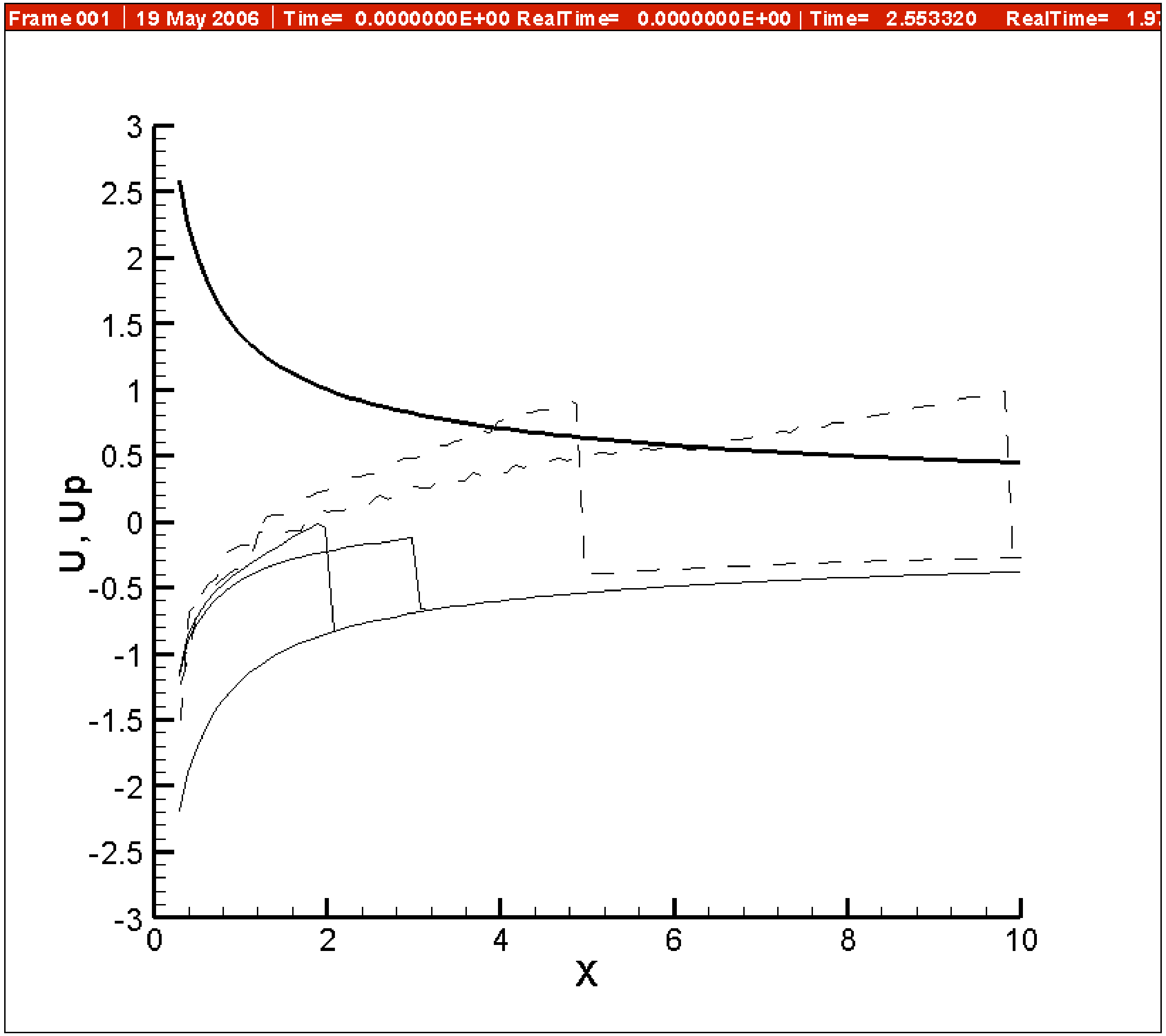
Frame 001 | 19 May 2006 | Time= 0.0000000E+00 RealTime= 0.0000000E+00 | Time= 2.553320 RealTime= 1.97
U, Up
X
3
2.5
2
1.5
1
0.5
0
-0.5
-1
-1.5
-2
-2.5
-3
0
2
4
6
8
10

$\square_0=1$

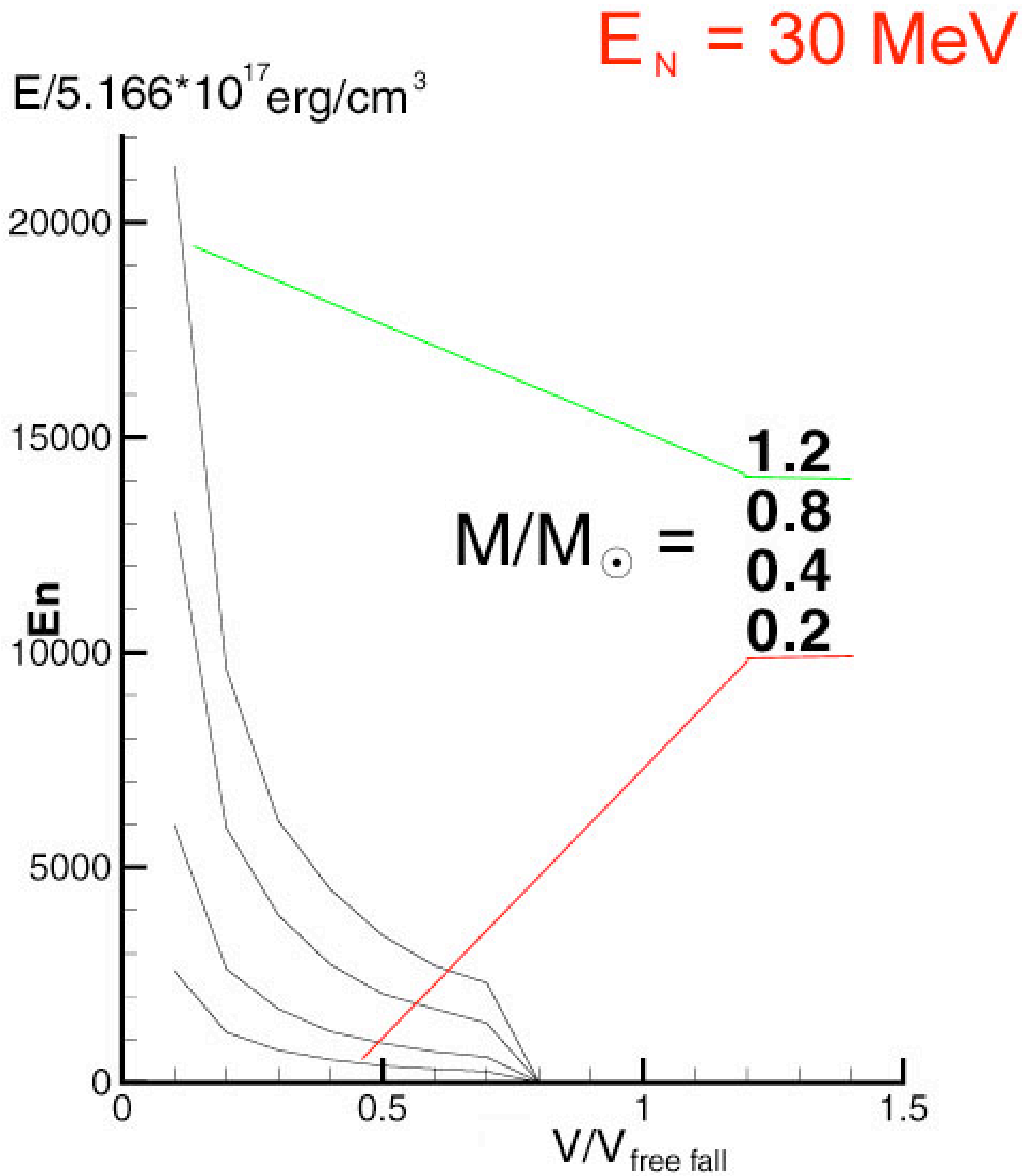

E N = 30 MeV
E/5.166*10^17 erg/cm^3
En
20000
15000
10000
5000
0
0
0.5
1
1.5
V/V free fall
M/M⊙ =
1.2
0.8
0.4
0.2

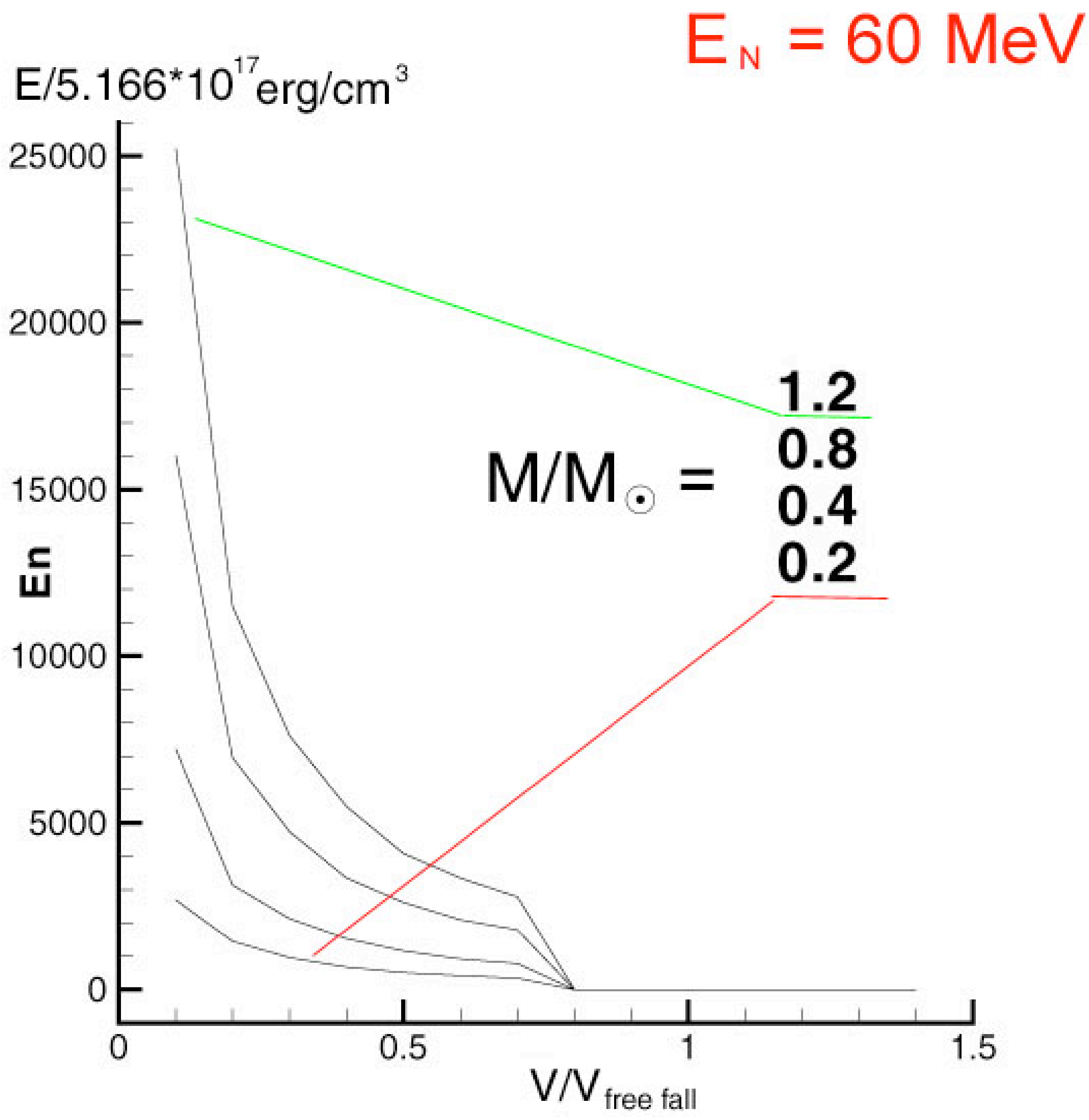

E_N = 60 MeV
E/5.166*10^17 erg/cm^3
En
25000
20000
15000
10000
5000
0
0
0.5
1
1.5
V/V free fall
M/M☉ =
1.2
0.8
0.4
0.2

Estimates of neutrino radiation

After 3.5 ms 0.02 _⊙ _ of this material approaches the boundary of the neutrino-sphere, where the density is _ = 10^{11} g/cm ^{3}, and becomes transparent to the neutrinos there. The density of these neutrinos is comparable to the density of electrons with mean energy 60 MeV. In this case, the intensity of the neutrino emission can be estimated as

$$L = (0.04\ \_\odot\ \mathbf{x}\ 60\ \mathrm{MeV})/(\_\ m_n\ \mathbf{x}\ 3.5\ 10^{-3}) \sim 4\ 10^{54}\ \mathrm{erg/s},$$

where _ is the mean molecular mass per electron in the absence of electron-positron pairs. We will now estimate the fraction of energy absorbed by matter per gram in the shock wave from this neutrino radiation. By definition, this is

$$\frac{d\varepsilon}{dt} = \varepsilon_\nu\ n_\nu\ n_t \langle \sigma v \rangle / \rho \approx L \sigma n_1 / \rho R^2\ erg\ g^{-1}\ s^{-1}$$

where R is the radius of the shock, $\sigma = g^2 \varepsilon_\nu^2 / \eta^4 c^4 \approx 10^{-44} (\varepsilon_\nu / m_e c^2)^2\ cm^2$ is cross-section of weak interaction, where g = 1.4102 ± 0.0012 10^{-49} erg cm^3 - constant Fermi of weak interaction, n_1 = 1.688 10^{28}, T_9^3 cm^{-3} is the density of $e^{\pm}$ in the shock wave when T corresponds an ultrarelativistic gas with _≤10^5 T_9^3 g/cm^3 . For T_9 = 100, _ = 10^8 g/cm^3 , and R = 10^7 cm, we obtain d_/dt = 0.97 10^{27} erg g^{-1} s^{-1} . This is much more than the neutrino losses from the shock front: d_ /dt ≈ 6 10^{10} T_9^6 ≈ 6 10^{22} erg g^{-1} s^{-1} ; i.e., the large-scale convection could support a diverging shock wave, leading to the ejection of the supernova envelope.

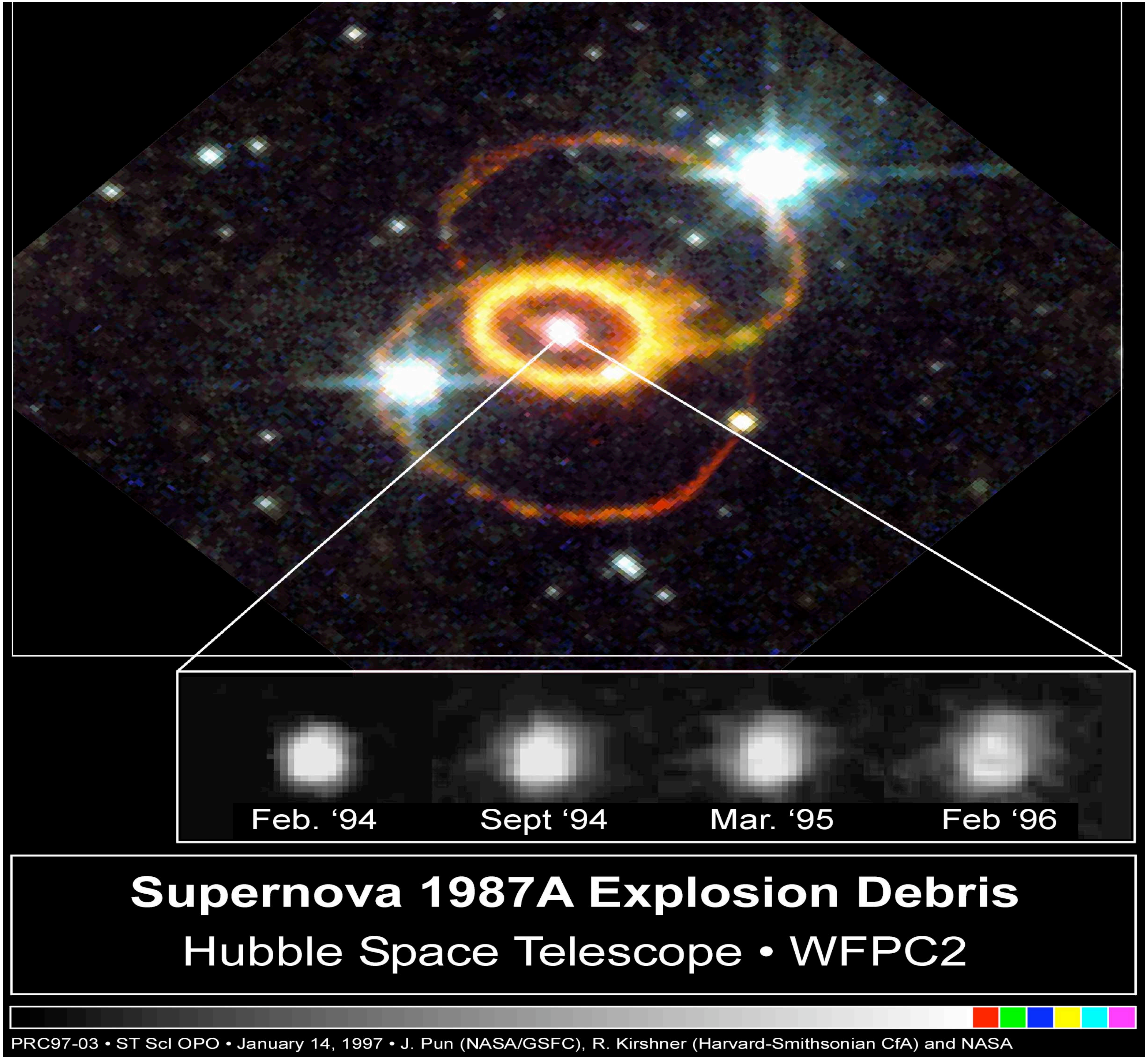
Feb. '94
Sept '94
Mar. '95
Feb '96
Supernova 1987A Explosion Debris
Hubble Space Telescope • WFPC2
PRC97-03 • ST ScI OPO • January 14, 1997 • J. Pun (NASA/GSFC), R. Kirshner (Harvard-Smithsonian CfA) and NASA

SN 1987A(1999 year)

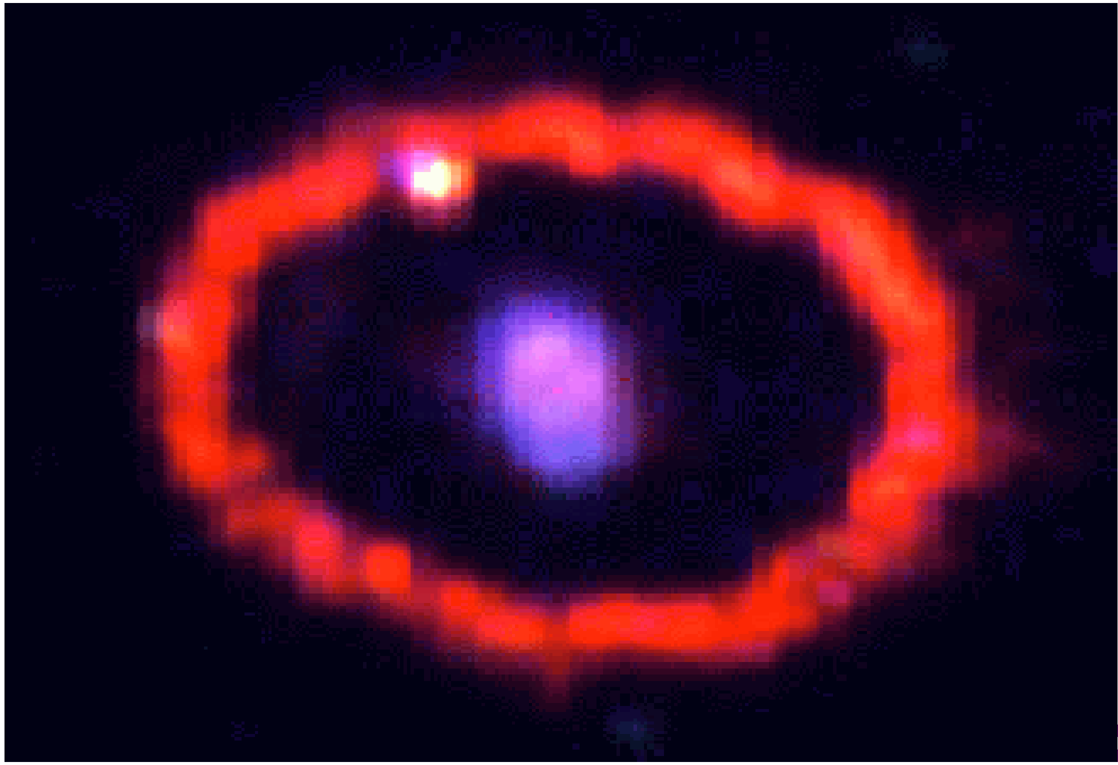

SN 1987A 1999

SN 1987A

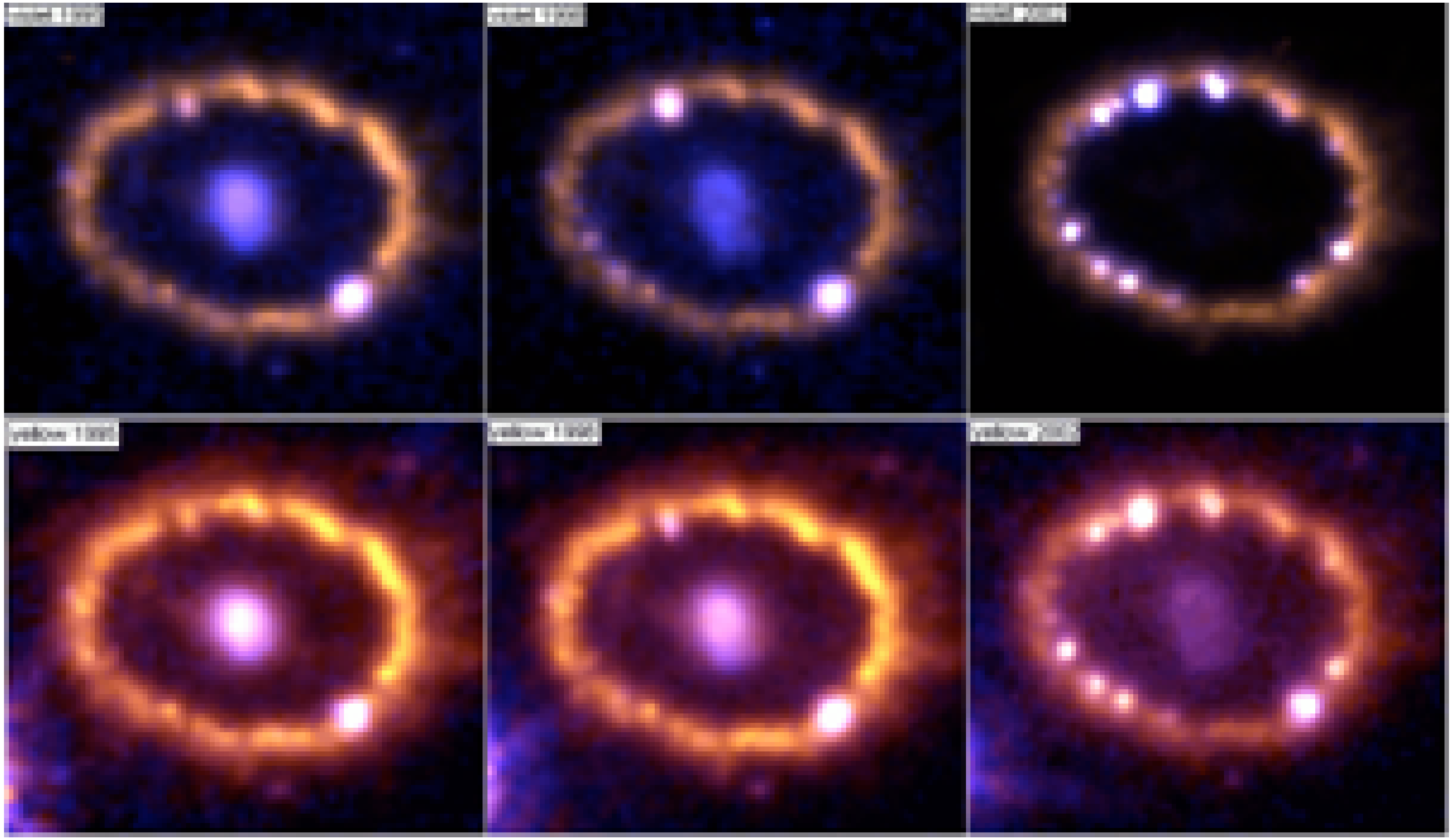

SN 1987A

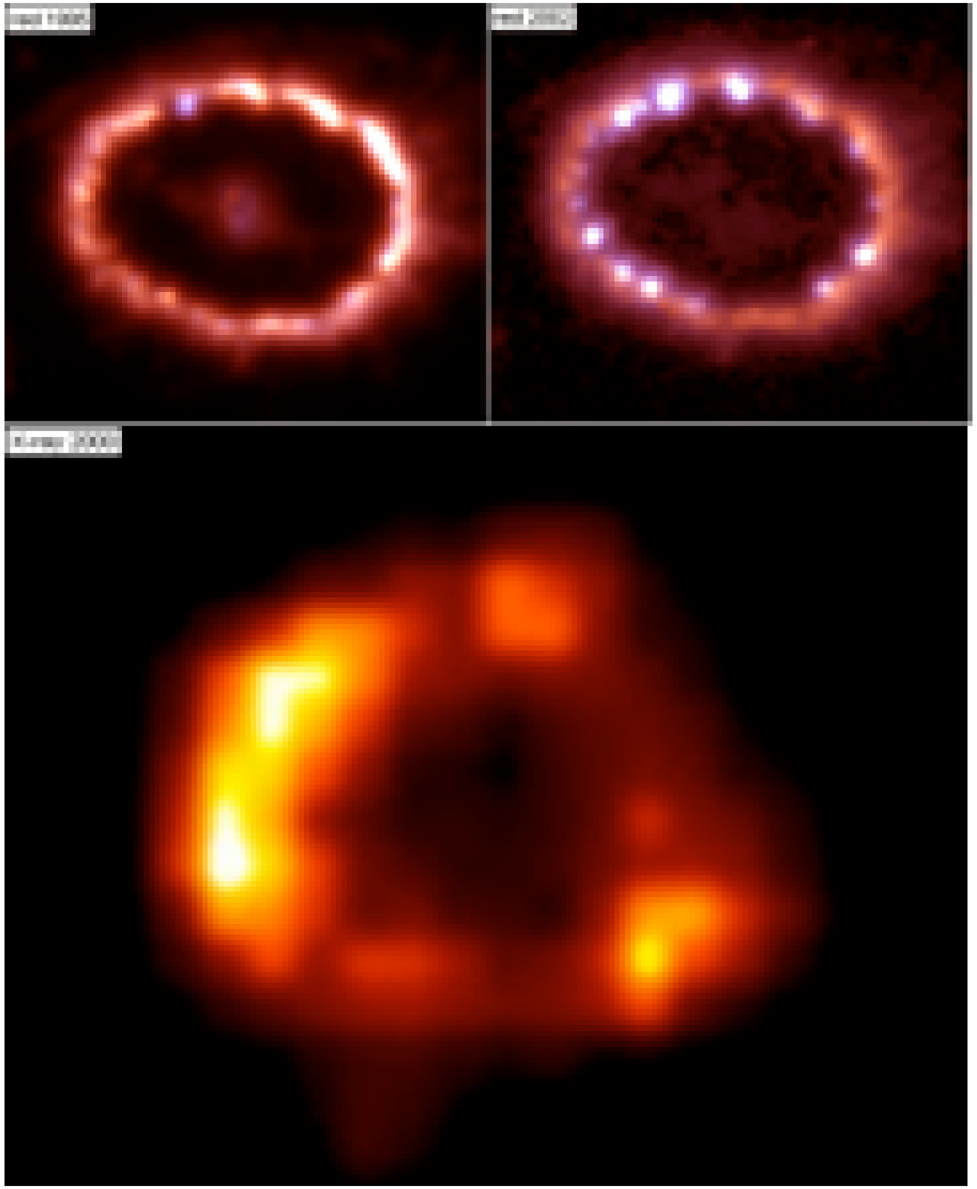

TYPES I AND II SUPERNOVAE AND THE NEUTRINO MECHANISM OF THERMONUCLEAR EXPLOSION OF DEGENERATE CARBON–OXYGEN STELLAR CORES

V. M. CHECHETKIN, S. S. GERSHTEIN, V. S. IMSHENNIK,
L. N. IVANOVA and M. Yu. KHLOPOV

Institute for High Energy Physics, Moscow, U.S.S.R.

(Received 21 May, 1979)

Abstract. The present work studies the hydrodynamic process of thermonuclear explosion of hydrostatic equilibrium, degenerate carbon-oxygen cores with $M_C = 1.40\ M_\odot$ with different values of central density ϱ_c within the interval $2 \times 10^9 < \varrho_c < 3 \times 10^{10}$ g cm^{-3}. The initial temperature distribution has been determined by the preceding thermal stage of explosion. The calculations successively include the kinetics of thermonuclear burning, the kinetics of β-processes, and neutrino energy losses. By considering the neutrino mechanism of heating and carbon ignition we obtained in our numerical hydrodynamic calculations two characteristic versions of the development of an explosion: (a) at $2 \times 10^9 < \varrho_c < 8 \times 10^9$ g cm^{-3} there is disruption of the whole star with either complete or partial burning of the carbon and a 10^{50}–10^{51} erg kinetic energy; and (b) at $9 \times 10^9 < \varrho_c < 3 \times 10^{10}$ g cm^{-3} the stellar core collapses into a neutron star with partial outburst of the outer envelope with a smaller kinetic energy of 10^{49}–10^{50} erg. The paper proposes and details a hypothesis (the scenario of supernovae and the formation of neutron stars) on the first version of explosion, corresponding to SN II, and on the second, supplemented by some mechanism of slow energy release into the envelope expelled from the newly formed neutron star, corresponding to SN I. On the basis of the proposed hypothesis a satisfactory agreement with the observed masses and energies of the supernovae envelope, their light curves and spectra, as well as with the data on their chemical composition has been obtained. For this agreement we must assume that type I pre-supernovae are almost bare compact carbon–oxygen stellar cores, and that type II pre-supernovae are red supergiants. It is most probable that the evolution of type I pre-supernovae occurs in close binaries while the evolution of type II pre-supernovae seems to be very similar to the evolution of a single star.

5. Astrophysical Applications and the Scenario of Supernovae Explosions of Both Types

We may now proceed to the astrophysical interpretation of the obtained results. The most important observational characteristics of supernovae are listed in Table II, from the summary of Chevalier (1977). To compare the theoretical results in Table I with the data in Table II we shall consider the following hypothesis (Gershtein *et al.*, 1977a, b): collapsing CO cores with ejection of the envelope (versions 1, 2 and 7, 8) will be assumed to be SNI; explosions of CO cores with a complete disruption of the star (versions 3–6) will be SNII. We shall first confine ourselves to a comparison of the first three lines of Table II. For SNII we can immediately state that there is good general agreement of the magnitudes M_e, $\bar{v}$ and E_{kin} ($E_{\mathrm{kin}} - M_e(\bar{v}^2/2)$), provided we take into account that a stellar CO core can be surrounded by an outer envelope with the mass $2.5 \lesssim M/M_\odot \lesssim 8.5$ (Barkat, 1975). It should be especially stressed that a very wide spread of the above-mentioned values is theoretically possible; this is also characteristic of observed SNII (Barbon *et al.*, 1974).

TABLE II

Magnitudes and properties	Supernovae	
	Type I	Type II
M_e (Envelope mass)	$0.5(0.1–1)\ M_\odot$	$> 5\ M_\odot$
$\bar{v}$ (Mean velocity)	10^9 cm s^{-1}	5×10^8 cm s^{-1}
E_{kin} (Kinetic energy of the envelope)	5×10^{50} erg	1×10^{51} erg
E_{ph} (Emission energy)	2×10^{49} erg	1×10^{49} erg
Population	Old population of the disk	Young population of the disk

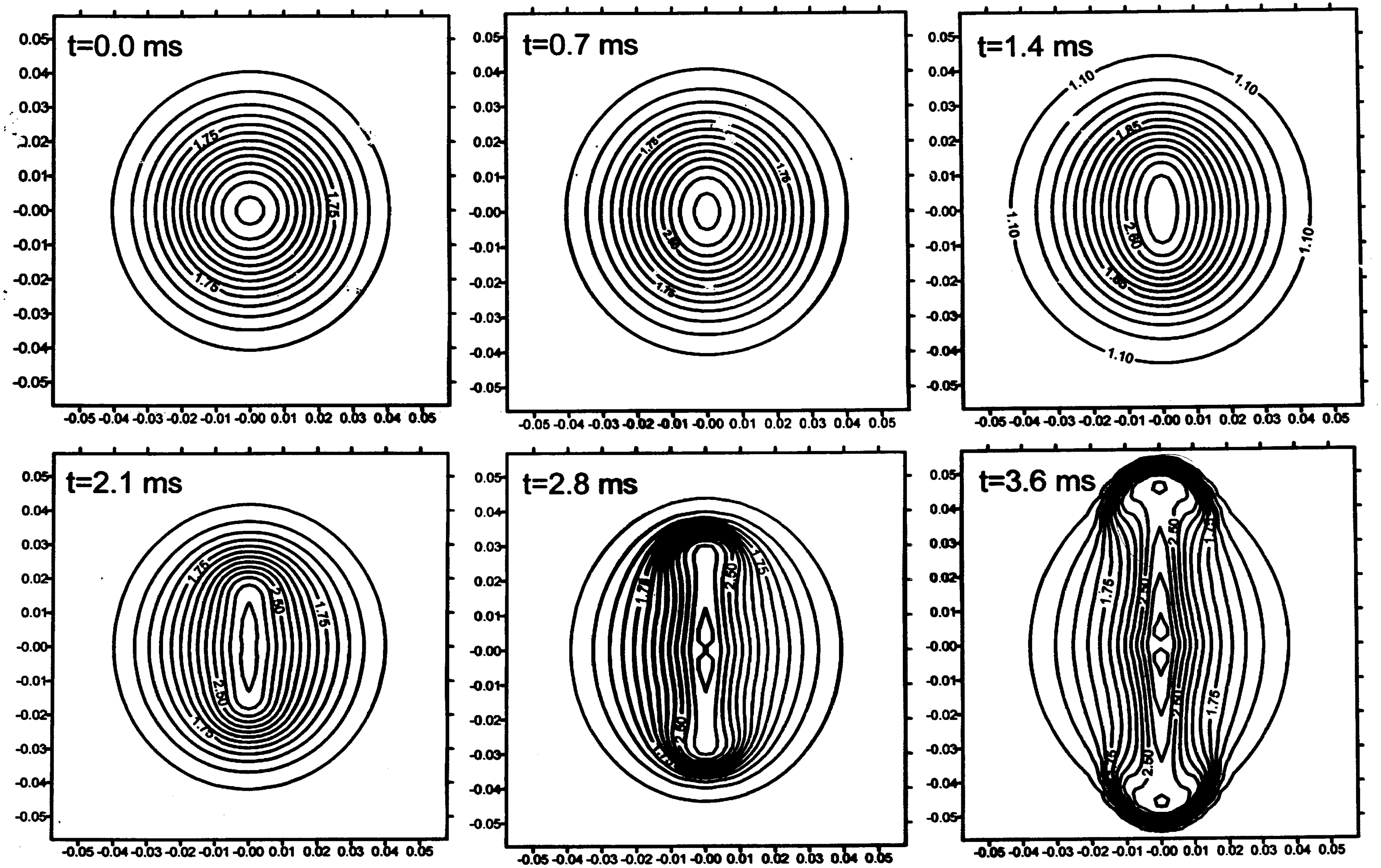

t=0.0 ms
t=0.7 ms
t=1.4 ms
t=2.1 ms
t=2.8 ms
t=3.6 ms

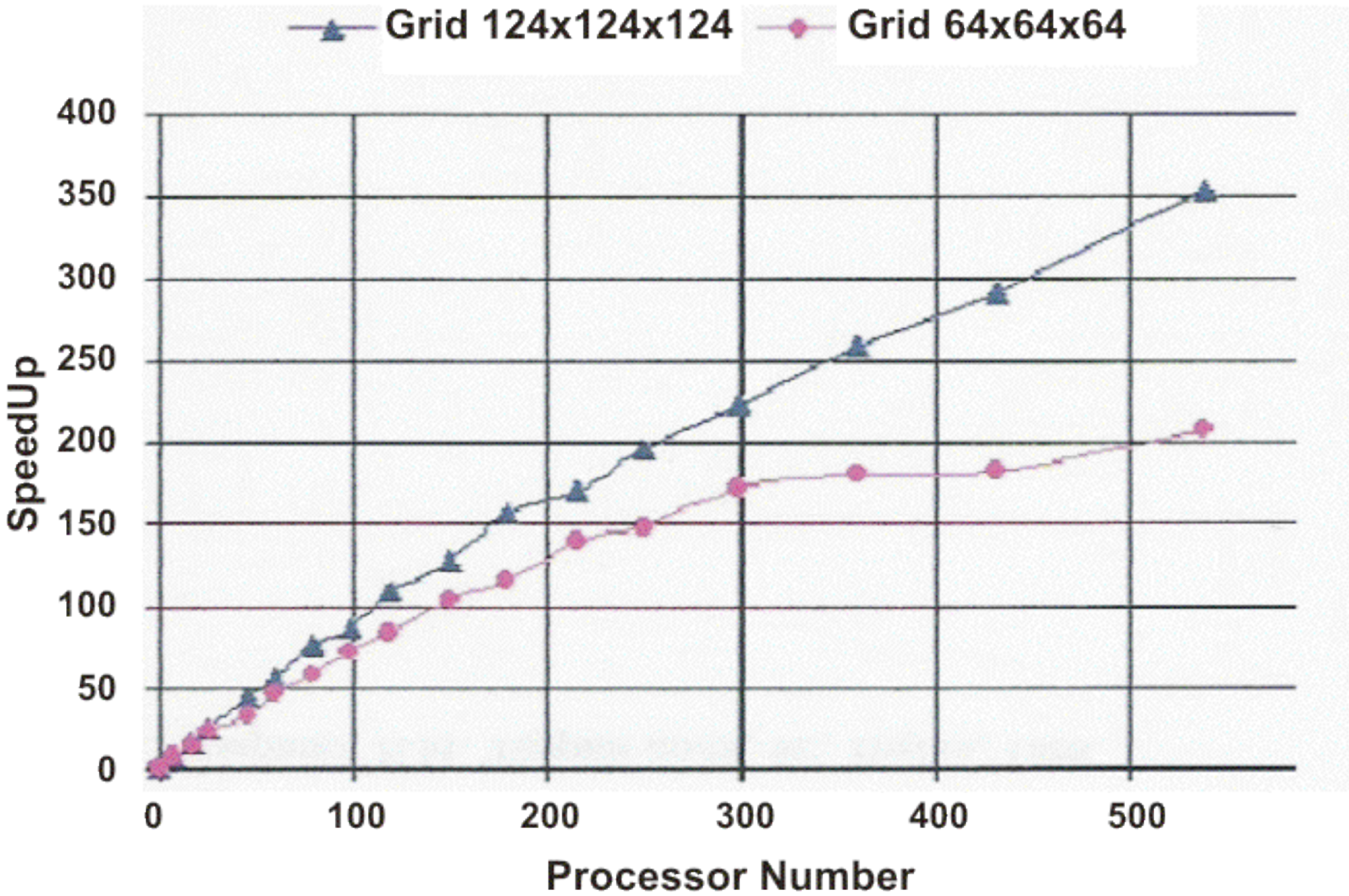

Grid 124x124x124
Grid 64x64x64
SpeedUp
400
350
300
250
200
150
100
50
0
0
100
200
300
400
500
Processor Number